Biological Cybernetics

Volume 46 Supplement 1983

W. Reichardt, T. Poggio, K. Hausen
Figure-Ground Discrimination by Relative Movement in the Visual System of the Fly. Part II: Towards the Neural Circuitry 1

Indexed in Current Contents — Covered by Zentralblatt für Mathematik

Springer-Verlag Berlin Heidelberg New York Tokyo

422 Biol. Cybern. ISSN 0340-1200 BICYAF 46 (Suppl.) 1-30 (1983)

March 1983

Biol. Cybern. 46, (Suppl.) 1–30 (1983)

Biological Cybernetics

Figure-Ground Discrimination by Relative Movement in the Visual System of the Fly

Part II: Towards the Neural Circuitry*

Werner Reichardt, Tomaso Poggio**, and Klaus Hausen
Max-Planck-Institut für biologische Kybernetik, Tübingen, Federal Republic of Germany

Abstract. A moving object can be separated from its surround on the basis of motion information alone. It has been known for some time that various species and especially the housefly can discriminate relative motion of an object and its background, even when the two have an identical texture. An earlier paper (Reichardt and Poggio, 1979) has analyzed on the basis of behavioural experiments the main features of the algorithm used by the fly to separate figure from ground. This paper (a) proposes the basic structure of a neuronal circuitry possibly underlying the detection of discontinuities in the optical flow by the visual system of the housefly *Musca*; (b) compares detailed predictions of the model circuitry with old and new behavioural experiments on *Musca* (measuring its attempts to fixate an object), and (c) studies the neuronal realization of the model circuitry in terms of electrophysiological recordings from the lobula plate horizontal cells of the blowfly *Calliphora*.

(a) The main features of the proposed circuitry are: 1) Binocular "pool" cells summate the output of a retinotopic array of small field elementary movement detectors covering the whole visual field and inhibit each ones of the detectors, which are then summated in output cells. 2) Inhibition is of the shunting type with an equilibrium potential very near the resting potential. 3) Saturation at the pool cells level together with nonlinear synaptic transduction (after shunting inhibition) provide a gain control mechanism which tends to make the overall response independent of the size of the motion field. 4) Forward as well as recurrent inhibition are possible and seem indistinguishable in terms of input-output experiments alone.

(b) The main results of testing the model predictions with behavioural experiments are: 1) Not only the time average of the fly's behavioural torque response but also its characteristic dynamics under different conditions of relative motions (oscillations of figure and ground texture with different phases and amplitudes) agree with the model predictions. 2) The behavioural optomotor response to moving fields is almost independent of the spatial extent of motion, but it depends on velocity, contrast and spatial structure of the image, as predicted by the circuitry. 3) The output of the circuitry closely mirrors the behaviour of the fly under a variety of binocular and monocular conditions (either ipsi- or contralateral for figure and ground). 4) The model is consistent with the fly's response even when instead of an object moving against a surround, two objects move each in front of a different eye.

(c) The electrophysiological figure-ground experiments on the horizontal cells in the lobula plate of *Calliphora* suggest that: 1) The horizontal cells have gain control properties consistent with the model's predictions. 2) The dynamics of the cell responses under various conditions of relative motion is consistent with the predictions of the circuitry for *Calliphora*. 3) There may be in addition to the horizontal systems additional neurons corresponding to the proposed circuitry, with different parameter values and correspondingly different gain control and visual field properties.

The relation between the skeleton circuitry proposed in this paper and its actual neuronal implementation is discussed in terms of the most likely physiological possibilities. It is shown that the circuitry implements a specific form of the general algorithm suggested from behavioural data in earlier papers. Finally, a computational analysis of the process im-

* We had planned a paper (cited as Part II in Reichardt and Poggio, 1979) about the visual algorithms used by the fly for computing movement and relative movement. We feel that the present paper, which studies the neural circuitry implementing these algorithms fulfills our previous goals. Another paper on more abstract algorithmic aspects of the movement and relative movement computations will appear elsewhere

** Present address: Massachusetts Institute of Technology, Dept. of Psychology, 79 Amherst Street, Cambridge, MA 02139, USA

plemented in the circuitry is outlined. It is suggested that object surround separation is based on the underlying assumption that discontinuities in the retinotopic array of the time dependent measurements provided by the movement detectors (more primitive than precise measurement of the optical flow) indicate the presence of an object (either because of relative motion or of different textures). The circuitry may even provide the starting point for developing efficient algorithms for early object surround separation in the computer analysis of time – varying imagery.

1. Introduction

The many uses of motion information are critically important for many biological systems and especially for fast flying animals like flies. Motion with respect to the visual world generates a distribution of apparent velocities on the eyes. Discontinuities in this "optical flow field" are a good indication of object boundaries and can be used to segment images into regions that correspond to different objects. The ability to uncover visual camouflage via relative motion certainly had a major role in one of the basic games played in the course of evolution, the competition between preys and predators. Sometimes, objects and targets can be identified by features independent of movement, like shape and colour. Often, however, motion is the simplest definitive feature.

Male flies may pursue passing objects in the assumption that one is a female of the same species. Colour, shape, and size play only a minor role; tracking or chasing is triggered and maintained by erratic relative motion between the relative image of an object and the surround (Land and Collett, 1974; Wehrhahn, 1979; Reichardt and Poggio, 1981; Wehrhahn et al., 1982). The irregular flight of flies will ensure that at least in certain instants the motion of the image of the leading fly across the retinae of the following fly will differ from the background. A tracking and also an early warning system may therefore effectively rely on the detection of relative motion. In general, the relative movement of an object against a surround can be used to reveal its presence and identify its boundaries. The human visual system is very efficient at exploiting this. Relative movements in random dot patterns, like the ones used in our experiments, yields a vivid perception of surface boundaries (Julesz, 1971; Regan and Spekreijse, 1970; Baker and Braddick, 1982). In everyday's life we continuously exploit our ability to isolate objects on the basis of motion information alone, for instance by inducing motion parallax through slight movements of our head. Somewhat similarly a fly can discover the relative retinal motion between a target and its background, even when the two are identical in texture and therefore indiscriminable in the absence of relative motion (Virsik and Reichardt, 1976; Heimburger et al., 1976). The ability to discriminate even stationary objects from a distant surround in terms of the relative velocity induced by their own motion is probably of special importance for fast flying insects which cannot rely on binocular vision.

In recent papers behavioural data on figure-ground discrimination by the fly have been used to characterize this computation, which is equivalent to the detection of discontinuities in the optical flow. We measured the torque response of a housefly to a textured small figure oscillating sinusoidally with a certain frequency and amplitude in front of a similar ground texture. The latter was also oscillated with the same frequency and a given relative phase in front of one or both compound eyes. It has been shown long ago that flies fixate, i.e. fly towards, a small contrasted object on a white background (Reichardt, 1973; Poggio and Reichardt, 1973; Reichardt and Poggio, 1976). Similarly, detection and discrimination of a figure in front of a ground is superimposed on the torque generaled in the usual optomotor response (which follows the oscillatory movement). Under our experimental conditions, the housefly optimally discriminates the figure for phase 90° and 270°. Detection decays from 90° (270°) to 180° (0°) where it is negligible (in the time averaged reaction). When the ground pattern is removed or at rest, the time averaged position-dependent response of the fly is probably due to both flicker detectors and asymmetric movement detectors, their relative importance being set by the time course of the stimulus. The analysis of the figure-ground experiments established that the corresponding algorithm relies on an inhibitory multiplication-like operation between those elementary movement detectors (possibly with flicker components) that are stimulated by the textured figure and those that respond to the ground. In the time-averaged responses obtained from experiments at 2.5 Hz oscillation frequency, this interaction is symmetric, i.e. movement from back-to-front (regressive) is equally effective as movement from front-to-back (progressive) in inhibiting the response to both progressive and regressive movement.

In this paper we derive and suggest the basic structure of a neuronal circuitry for relative movement discrimination by the visual system of the fly *Musca domestica*. The proposed circuitry is based on quantitative behavioural experiments. In the previous analysis we were restricted to the time averaged behavioural responses whereas the present analysis rests

to a large extent on the dynamics of the torque response and on new physiological data. The conjectured neural circuitry has been recently outlined in a preliminary note (Poggio et al., 1981). The organization of the paper is as follows: after a description of the behavioural and physiological methods (Chap. 2), we outline several key experiments which provide particularly critical constraints on a neuronal model (Chap. 3). Some of the biophysical mechanisms hypothesized for the circuitry and the main mathematical problems are dealt with in Appendices A and B, respectively. A comparison between the predictions of the theory and many old and new behavioural experiments with *Musca* is the subject of Chap. 5. Electrophysiological data on lobula plate neurons, possibly corresponding to some components of the model circuitry, are introduced in Chap. 6. Since for technical reasons the recordings were performed on the fly *Calliphora*, comparative behavioural experiments were also carried out. The discussion (Chap. 7) deals with a number of critical issues which can be broadly divided into two categories. The first set of questions deals with the relation between the proposed circuitry, its actual neuronal implementation and the interpretation of experimental data. The second part sketches the outlines of a computational theory of the visual process performed by the circuitry. It suggests that the circuitry, considered as an algorithm solves a nontrivial problem for computer vision. Finally, the specific structure of the corresponding algorithm is related to the role of figure-ground separation for the fly.

2. Experimental Procedures, Material and Methods

2.1. Behaviour

Behavioural experiments in our laboratory have dealt with the registration of flight tracks of freely flying flies as well as with the measurements of dynamic and time averaged responses under restricted and controlled conditions.

In free flight a fly has, in addition to head movements, six dynamic degrees of freedom; three of translatory and three of rotatory motion (without considering the additional degrees of freedom associated with head movements etc.). Registration techniques developed for the testing of freely flying flies have reached a resolution which enables us to resolve five of the six degrees of freedom whereas servotransducers allow us to measure responses of fixed flying flies for one of the degrees of freedom each at a time. These transducers either sense the flight torque or the lift and thrust forces generated by the wings of an individual test fly.

Since the head of the fly is fixed in the experiments reported here to the thorax, a resting pattern represents a stabilized retinal image for the test fly (see Reichardt, 1973). Contrasted environments (ground and figure) were provided by statistical patterns with pixels (either black or white) of $3° \cdot 3°$ (Julesz patterns), mounted on two concentric cylinders. In Fig. 1 the technique used in the experiments is shown in a schematic diagram.

In the figure-ground behavioural experiments, described in this paper, the figure (either a black or random-dot textured, vertically oriented stripe) was oscillated around a position $\psi = +30°$, where ψ is the horizontal angle in the equatorial plane of a fly; $\psi = 0°$ designates the symmetry direction between the two compound eyes. In most experiments the textured ground was oscillated sinusoidally. The oscillation frequencies of figure and ground amounted to 2.5 Hz, the oscillation amplitudes are stated in the legends of the figures. The torque response generated by a test fly was stored in an averager (Princeton Signal Averager Model 4202) and plotted after the test. The number of sweeps stored in the averager per experiment amounted to 100, if not stated otherwise. The computer simulations were carried out with an Hewlett-Packard 9826 computer. The behavioural experiments were performed on female, wild type *Musca domestica* and *Calliphora erythrocephala* from our laboratory stock.

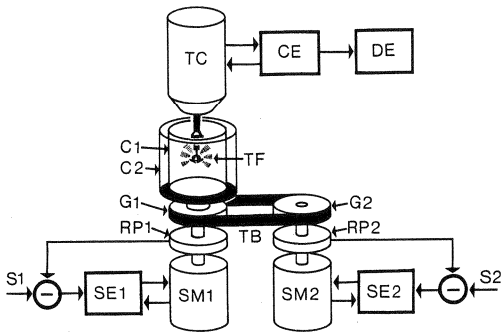

Fig. 1. Schematic representation of the experimental set-up used in the behavioural experiments described in this paper. A test fly TF is suspended from a torque compensator TC which is connected to the compensator electronics CE. The voltage output of CE is proportional to the torque signal generated by the fly under compensation. The CE output is evaluated by a data evaluation device DE. For on line data evaluation we used a Princeton Signal Averager Model 4202. The motion of two cylinders C1 and C2 is controlled by two 400 Hz servomotors SM1 and SM2 whose shafts carry ring potentiometers RP1, RP2 and gears G1 and G2. The inner cylinder is connected with the servomotor SM1 whereas the outer cylinder is driven by a transmission belt TB from servomotor SM2. The ring potentiometer voltages are fed back to the inputs of the servomotor electronics SE1 and SE2, so that SM1 and SM2 are operated under position control from the inputs S1 and S2, respectively. Under these conditions an angular displacement of a cylinder is strictly proportional to the voltage S applied to an input of the SE electronics. The two cylinders are illuminated by four DC current driven fluorescent ring bulbs (not shown). The average brightness at the surface of the cylinders amounts to about $700\,\mathrm{cd} \cdot \mathrm{m}^{-2}$. (From Reichardt and Poggio, 1979)

2.2. Electrophysiology

Electrophysiological experiments were carried out with female blowflies *Calliphora erythrocephela*, aged 3–10 days, from the stock of the institute. For recording, the test animal was immobilized and the rear of its head capsula was opened in order to expose the lobula plate of the right optic lobe. The equatorial horizontal cell of this neuropil was recorded intracellularly. The measured graded signals were averaged using a Princeton Signal Averager Model 4202. The electrophysiological technique is described in detail elsewhere (Hausen, 1982a, b).

In the experiments the flies were adjusted to the center of the stimulus setup identical to that described above, except that the ground panorama was opened behind the fly in order to allow access to the animals with micromanipulators and electrodes. The cylindrical ground panorama reached from $-105° \leqq \psi \leqq +105°$; the figure was positioned in the right visual field at $\psi = +40°$ and had a width

of 10°. Figure and ground were oscillated sinusoidally with a frequency of 2.5 Hz and an amplitude of ±5°. If not stated otherwise, relative motion stimuli were displayed in a standard stimulus program which consisted of 3 subsequent intervals: (a) synchronous motion of figure and ground (5 s), (b) relative motion of figure and ground (5 s; phase between figure and ground motion set to either $\phi = 0°$ or 90°, 180° or 270°), (c) stationary pattern (2 s). The recordings shown in this paper represent response-averages of the equatorial horizontal cell obtained from 20 repetitions of the stimulus program and contain in each case the last period of synchronous motion for reference and the subsequent 3 periods of relative motion.

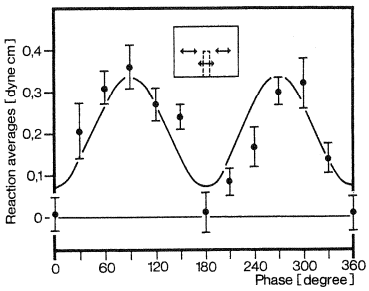

Fig. 2. Phase dependence of the figure-ground discrimination effect. Average torque responses of ten flies to sinusoidally oscillating figure and ground patterns. The figure consists of a black, vertically oriented stripe, 3° wide, positioned in the lower part of the panorama, oscillated around the mean positions $\psi = \pm 30°$. The ground pattern consists of a random-dot texture which can be moved independently from the stripe. A white stationary screen (12° wide) is mounted between the stripe and the ground pattern in order to avoid mixed stimulations of receptors by the stripe and by the ground. The oscillation amplitude of stripe and ground were ±1° at 2.5 Hz frequency. The vertical bars denote standard errors of the mean. The continuous line is the component $k_4 \cdot \cos(2\phi)$ derived from a Fourier analysis of the data plotted in the figure. The inset of the figure indicates the stimulus conditions. Each point is an average from 10 flies. (From Reichardt and Poggio, 1979)

3. Key Experiments

As we stated before, flies can detect an object against a textured background, provided these move relative to each other. The same behaviour can be observed when the object is replaced by a textured figure if the textures of figure and ground are statistically equivalent. The "figure" and "ground" discrimination had been at first demonstrated in a series of closed-loop experiments (Virsik and Reichardt, 1974, 1976). Under closed-loop conditions, a fly suspended by the torque compensator controls by its own torque signal the angular velocity of a ground texture and of an object in front of the ground. If there is even a very small relative motion between object and ground, the fly is able to fixate and track the object. Open-loop experiments where the fly does not control the motion of its optical environment demonstrate the same effect (Poggio and Reichardt, 1976).

In a previous analysis (Reichardt and Poggio, 1979) we restricted ourselves to time averaged behavioural responses and characterized the algorithm underlying for figure-ground discrimination. A typical figure-ground test where the time averaged response is plotted as a function of the phase between oscillating figure and oscillating ground is shown in Fig. 2. As has been already mentioned before, the fly optimally discriminates the figure from the ground for relative phase angles $\phi = 90°$ and 270°.

3.1. Binocular Experiments

A first set of time dependent experiments is presented in Fig. 3a–c. The experimental procedure is the following: A flying fly is fixed in space by the torque meter shown in Fig. 1 and its torque around the vertical axis is recorded as a function of time and averaged over a number of periods. Positive (negative) torque means that the fly tries to turn to the right (left). The animal is stimulated by a small figure (a vertically oriented and textured stripe of 12° width) sinusoidally oscillated at 2.5 Hz frequency around a position $\psi = +30°$. A random-dot textured ground (a Julesz pattern of the same texture as the figure) is also oscillated with the same frequency and a phase ϕ, relative to the oscillating figure. The lower part of the figure indicates the positions (not the velocities) of figure and ground as functions of time. The oscillation amplitudes of figure and ground are equal and amounted in these experiments to ±5°.

The response plotted in Fig. 3a consists of an initial part in which the phase between figure and ground oscillation is 0°, followed by a part in which the phase has been switched to 90°. In the phase 0° region the test-fly generates an oscillatory response around zero torque. At time 0.4 s, phase ϕ is switched to 90° and subsequently the response increases, reaching a positive level around which it oscillates in a rather complex fashion: an increase in the responce is followed by a kind of plateau and a sharp peak. When the phase relation between figure and ground amounts to $\phi = 90°$, the time average of the response is positive, i.e. the fly is attracted by the oscillating figure. This finding agrees with our earlier experiments (shown in Fig. 2) in which we measured only the time average of the response. The time course of the response contains important information about the underlying neural circuitry.

A similar result is found when the relative phase between figure and ground amounts to $\phi = 270°$ as shown in Fig. 3b. The phase shifts again from 0° to 270° after 0.4 s. The response reaches a positive level and oscillates around it in a fashion which is the mirror image of the plot shown in Fig. 3a. The peak is followed by a kind of plateau which is then followed by a declining response. Since the time average is positive,

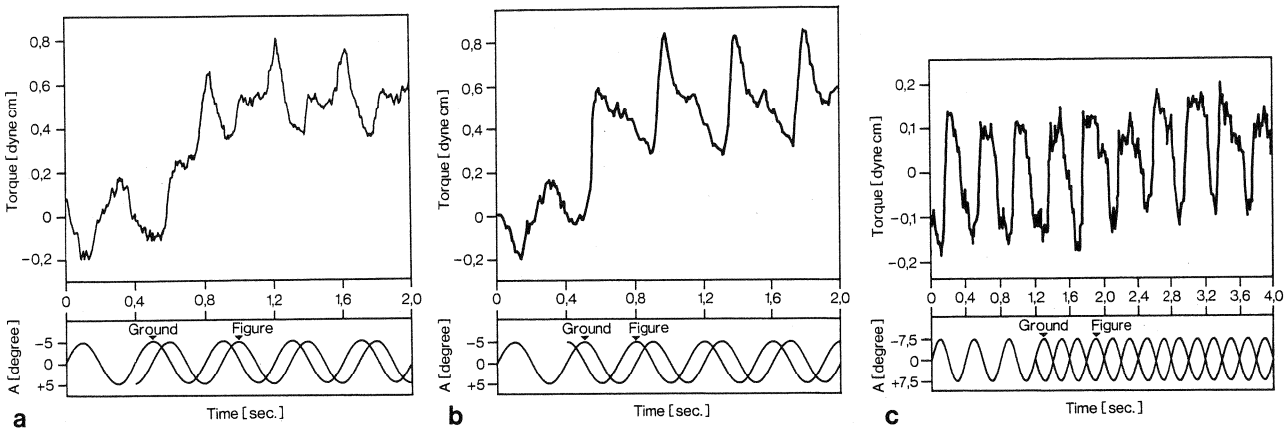

Fig. 3. a A typical response of a test fly in a bilateral figure-ground experiment. A textured stripe of 12° angular width is sinusoidally oscillated in front of a 360° textured background which oscillates with the same amplitude and the same frequency (2.5 Hz). The stripe oscillates around the mean position $\psi = +30°$ that is in front of the right eye. Oscillation amplitudes amount to $\pm 5°$ and $\pm 7.5°$ in **c**. The time courses of the figure and the ground oscillations (in terms of positions) are plotted in the lower part of the figure. With regard to the right compound eye, movement from $-5°$ to $+5°$ are progressive movements, whereas movements from $+5°$ to $-5°$ are regressive movements. At time 0.4 s the relative phase between figure and ground switches from 0° to 90°. The response (torque) of the fly increases after the phase has shifted and oscillates around a positive average response level with 2.5 Hz frequency. The increase of the response means that the fly is attracted by the oscillating figure. Each period of the response consists of three phases: a kind of plateau, a peak and a phase below the plateau level. The response plotted is an average of 100 sweeps. **b** All parameters as specified in the legend of **a**, except that the relative phase between the oscillating figure and the oscillating ground amounts to 270°. Again the fly is attracted by the oscillating figure after the phase has changed (at time 0.4 s). The time course of an oscillation of the response is reversed with respect to the 90° phase situation. A peak is followed by a plateau and a part below the plateau level. **c** All parameters as specified in the legend of **a**, except that the relative phase between the oscillating figure and the oscillating ground shifts from 0° to 180° at time 1.2 s. The response of the fly is oscillatory with no phase shift observable after the figure-ground phase has changed from 0° to 180°

the fly is attracted by the oscillating figure, again in accordance with our earlier findings (see Fig. 2). Finally, Fig. 3c shows the torque response to the relative phase $\phi = 180°$. The response is periodic without any indication of a phase change after time 1.2 s when the phase has shifted from 0° to 180°. The time averaged response is zero (for the entire test, not shown in the figure) at phases $\phi = 0°$ and $\phi = 180°$. For $\phi = 0°$ the result is of course trivial, but not so for $\phi = 180°$.

3.2. Monocular Experiment

Interestingly, figure-ground discrimination is not only confined to conditions where the figure moves in front of the ground texture. "Discrimination" is even observed when the figure oscillates in front of one compound eye and a half ground (180° wide texture) in front of the other compound eye (contralateral condition). A typical example of a contralateral figure-ground experiment is presented in Fig. 4. The parameter settings are here as described in connection with the preceding experiments. Figure and half ground oscillate initially in synchrony; the phase shifts to 90° at time 1.2 s. Throughout the experiment the response is negative since a much larger area in the left eye is stimulated than in the right eye. The fly's response clearly decreases (indicating a turning tendency towards the oscillating figure) when the phase between figure and ground changes from 0° to 90°. The observation leads to the conclusion that figure-ground discrimination is a binocular phenomenon in the sense that interactions between the two compound eyes are critically involved.

The experiments reported so far demonstrate the figure ground discrimination effect under bilateral and contralateral stimulus conditions for various relative phases between movements of figure and ground. Throughout the experiments parameters like oscillation amplitude, frequency of oscillation and angular width of figure were not changed.

3.3. Gain Control

In the following set of experiments we investigated the influence of the width of the figure on the response of the fly. These experiments turned out to be surprisingly relevant to an understanding of the figure-ground discrimination process at the cellular level. The first hint for the importance of the parameter figure's width came from a closer inspection of the figure-ground response at 90° phase shift, as shown in Fig. 3a. It is clear that a figure oscillating in front of a ground texture has a dramatic effect on the fly's behaviour when oscillated at 90° or 270° phase shift even for very small figure widths. The argument is based on the following quantitative considerations: A Fourier-

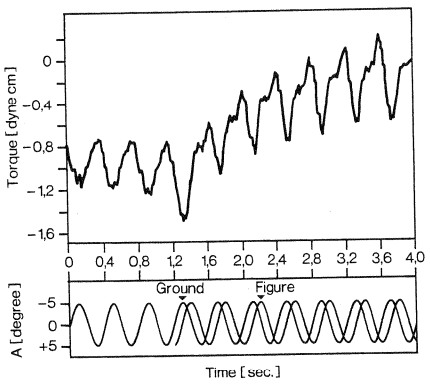

Fig. 4. A contralateral figure-ground experiment. All parameters as specified in the legend of Fig. 3a, except for the angular extension of the ground. The textured ground covers only 180° and extends from $\psi = 0°$ to $\psi = -180°$. It therefore stimulates the left compound eye whereas the figure oscillating around $\psi = +30°$ stimulates the right compound eye. The edges of the oscillating ground are covered by 10° wide screens. The response of the fly is oscillatory and decreases when the phase of the oscillating figure and ground changes from 0° to 90°. That is to say, even under these conditions, the figure is discriminated and the fly attracted by the figure when the phase is 90°. Note that the average response levels are negative. This is due to the fact that the ground texture stimulates only one of the two compound eyes. The plot is an average from 100 sweeps

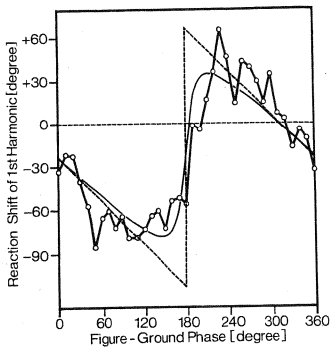

Fig. 5. Phase-phase plot derived from stationary data plotted like those shown in Fig. 3a. One response period to figure-ground oscillations at various relative phase angles is Fourier analyzed and the phase of the first harmonic relative to the ground phase is plotted against the figure-ground phase. For more details see text

analysis of a period of the stationary part of the response in Fig. 3a (when the figure-ground phase amounts to $\phi = 90°$) yields a phase shift against the relative figure-ground phase, as shown in Fig. 5. The other in the phase-phase relation are computed from other figure-ground experiments with different figure-ground phases. At figure-ground phase 0°, the torque response of the fly is delayed in phase against the oscillatory motion (frequency 2.5 Hz) of figure and ground by about −30°. Actually the phase lag amounts to $90° + 30° = 120°$ at this frequency as the optomotor response of the fly to an oscillating texture is a response to the velocity of the pattern and not to its position. Indeed for very low oscillation frequencies the response leads by 90° with respect to the instantaneous position of the oscillating texture. When the figure-ground phase is increased, the phase lag of the first harmonic of the response also increases. It reverses its direction at and above 180° figure-ground phase and returns to −30° phase lag when the figure-ground phase reaches 360°. Let us now make the following "Ansatz", concerning the first harmonic component of the oscillatory torque response to the oscillations of figure and ground: The figure's oscillation is given by the expression $A \cdot \sin(\omega t + \phi)$ and the ground's oscillation by $B \cdot \sin(\omega t)$ with ϕ, the relative phase between the two oscillations. $C \cdot \sin(\omega t + \vartheta)$ describes then the first harmonics of the fly's response to the oscillations of figure and ground. If the response is in first approximation a linear combination of the influence of figure and ground, then $C \cdot \sin(\omega t + \vartheta) = A \cdot \sin(\omega t + \phi) + B \cdot \sin(\omega t)$. The relation between ϑ and ϕ is given by the following expression

$$\operatorname{tg}\vartheta = \frac{\sin\phi}{\frac{B}{A} + \cos\phi}. \qquad (1)$$

When $A = B$, the relation between ϕ and ϑ corresponds to the dashed curve in Fig. 5 whereas the other curve corresponds to $A/B = 1.2$[1]. The experimental data plotted in Fig. 5 indicate that the influence of the oscillating figure on the torque response is of the same order as the influence of the oscillating ground although the angular extent of the figure is only a fraction of the 360° extent of the ground. It seems therefore plausible that some kind of automatic "gain control" is responsible for a normalization of the response to the oscillating figure as to the oscillating ground.

Even more convincing than the arguments given above is an experiment plotted in Fig. 6. Figure and ground are oscillated in synchrony (0° phase). The oscillation of the ground is stopped at time 0 s and switched on again at time 12 s. The response of a test fly increases strongly – the fly is attracted by the oscillating figure – reaches a stationary value and drops to the original value when the ground's oscillation is switched on again. Measuring the oscillation amplitude in the two stationary phases of the response one concludes that they are about equal; a finding which agrees with the observation we have discussed before. The oscillatory response elicited by the oscillating small figure is about the same as the oscillatory response elicited when figure and ground oscillate together in synchrony.

1 The relation between ϕ and ϑ in Eq. (1) is fitted to the experimental data (shift of ϑ to negative values for $\phi = 0$). The figure-ground phase in the experiments has a negative sign

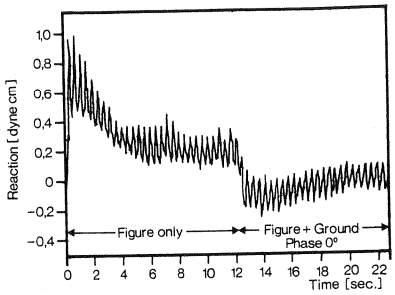

Fig. 6. Figure-ground experiment. Prior to the start of the recording, figure and ground are oscillated in synchrony. At time 0 the ground stops oscillating whereas the figure continues to oscillate. At about time 12 s the ground starts oscillating again in synchrony with the figure. Parameters: Oscillation frequency of figure and ground 2.5 Hz; oscillation amplitude of figure and ground $\pm 5°$; position of the figure $\psi = +30°$, angular extent of the figure 12°, angular extent of the ground 360°. After the ground stops oscillating, the fly is strongly attracted by the figure. The attraction response reaches a stationary level after about 5 s. The response drops to zero level when figure and ground are oscillated together. The amplitudes of response oscillations during the stationary period when only the figure is oscillating or when figure and ground are oscillating together are about equal. The outcome of this experiment is that the fly's response oscillations are almost independent from the dimensions of the pattern, suggesting a specific gain control mechanism. The plot is an average from 100 sweeps

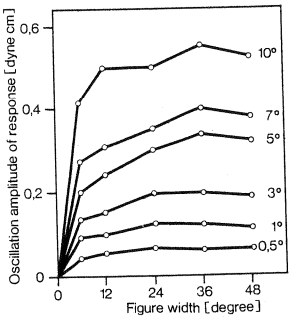

Fig. 7. Oscillation amplitude of the torque response as function of the angular extent of the figure (0°–48°) and the oscillation amplitudes of figure and ground (0.5°–10°). Experimental procedure as described in the legend of Fig. 6; plotted is the oscillation amplitude of the fly's response during the stationary response phase when only the figure oscillates. Parameter is the oscillation amplitude of the figure. For a given amplitude of the oscillating figure, the amplitude of the response increases with increasing figure width but reaches a rather constant level as soon as the figure's extent amounts to more than 12°. Each point derived from 100 measurements

These results have prompted us to measure the oscillation amplitude of the torque response under the same conditions as described in Fig. 6 as a function of the figure's width. Parameter in these experiments is the amplitude of the oscillating figure. The results of the measurements are shown in Fig. 7. They indicate that response amplitudes are rather independent from the width of the oscillating figure, but increase when the amplitude of the oscillating figure is increased. It

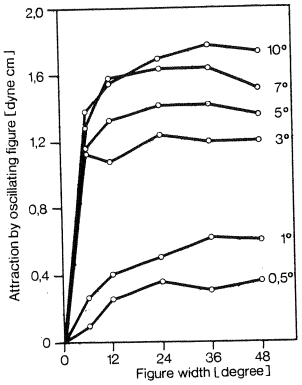

Fig. 8. Mean torque response (attraction) as a function of the figure-width (0°–48°), the parameter being the oscillation amplitude (0.5°–10°). Experimental procedure as described in Fig. 7. Whereas in Fig. 7 we have plotted the oscillation amplitude of the response, here we have plotted the attraction of the fly towards the oscillating figure as function of the figure's width. Parameter of the plot is again the oscillation amplitude of the figure. The result is similar as in Fig. 7. The response is nearly independent of the angular extent of the figure's width. It however increases, like in Fig. 7, with increasing oscillation amplitude of the figure. Each point derived from 100 measurements

should be added here that an increase in amplitude means an increase in velocity as well as an increase in the number of stimulated receptors. Not only the amplitude of the dynamic response but also the average response of the fly (the "attraction" toward the oscillating figure) behaves in accordance with a gain control mechanism (see Fig. 8).

In summary, the time course of figure-ground experiments with oscillating figures and oscillating grounds suggest that a small figure is about as effective as the ground. This observation is supported by response measurements to oscillating figures with different angular extensions. The experiments strongly suggest that the response depends on a gain control mechanism that operates on the width of the oscillating figure, or more precisely on the number of detector channels excited by the figure.

4. Outline of a Cellular Theory

In the preceding chapter we have shown that the dynamics of the fly's torque response is a characteristic signature for every specific phase condition in a typical figure-ground experiment. The figure-ground discrimination effect is observed not only under normal binocular conditions when the ground texture covers 360° and the oscillating figure stimulates one compound eye; surprisingly the effect is observed also under contralateral conditions when the figure stimulates one eye and the ground texture the other eye.

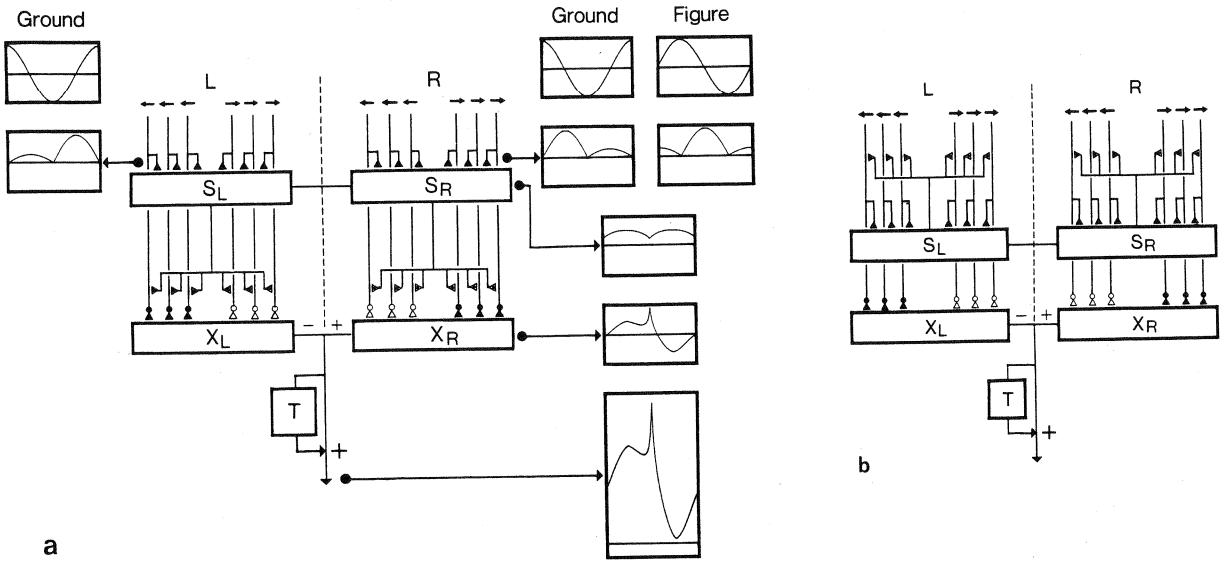

Fig. 9. a The outline of the model circuitry for the right (R) and for the left (L) eye. Considering the right eye as example, two retinotopic arrays of elementary movement detectors, responding selectively to progressive (→) and regressive (←) motion, serve as input channels to the neural circuitry. The two arrays share the same field of view. For convenience they are drawn apart from each other. A pool neuron (S_R) summates the detector outputs (—◂ indicate excitatory synapses) as well as the input from its contralateral homologue (S_L). Its output is assumed to undergoe a saturation effect (modeled by taking the square root of its overall excitation) and to shunt each elementary movement detector output via presynaptic inhibition. The synapses involved (—◂) should therefore inhibit (opening ionic channels with an equilibrium battery close to the resting potential) the output terminal of each elementary detector channel. The output cell X_R summates the progressive (excitatory, —◂) and the regressive (inhibitory, —○◂) detectors. Progressive channels have a higher amplification than regressive ones, possibly because of the different ionic batteries involved. The synapses on the X_R cell are assumed to operate with a nonlinear input-output characteristic, leading to postsynaptic signals that are approximately the square of the inputs. The motor output is controlled by the X-cells via a direct channel and a channel T computing the running average of the X-cells output. The insets in the figure contain the responses at the various levels to a bilateral figure-ground experiment with a relative phase of $\phi = 90°$ (see text). Responses at the input channels are split into two components, the ground component and the figure component. The process of shunting inhibition is described in Appendix A, whereas the mathematics of the circuit is discussed in Appendix B, first part. **b** The outline of another neural circuitry that can also explain the behavioural responses at the cellular level. The model is a recurrent shunting inhibition network. The important difference between the two models is that the first one (**a**) contains a shunting inhibition pathway acting on the channels after the pool cells (S) have received the detector signals – that is to say the pool acts forward. In the model presented here the pool operates via a recurrent pathway that acts on the individual detector channels before receiving signals from the individual channels. The recurrent network may become unstable (see Appendix B). All other details as described in the legend of **a**

The torque response of the fly follows the oscillation of a given pattern, as it is well known from studies of the optomotor behaviour. Our experimental data convincingly show that the amplitude (and speed) of the response increases with the movement amplitude whereas it is almost independent from the dimensions of the pattern, suggesting a specific gain control mechanism.

The experiments reported so far have prompted us to develop a neural circuitry implementing the figure-ground discrimination algorithm and obeying the following constraints: 1) The circuitry should provide a gain control mechanism for the overall optomotor reaction. 2) The inhibitory, nonlinear interaction is realized through large field movement-selective neurons inhibiting elementary movement detectors. 3) The neural model should produce the characteristic dynamics of the torque response for all phases between figure and ground and for the various types of stimulations.

A neuronal circuitry satisfying these constraints is outlined in Fig. 9a. The circuitry receives channels from a retinotopic array of elementary movement detectors as its input[2]. Each channel carries output signals from one and only one movement detector. The usual assumption was made that all cells carry only positive signals: in particular, detectors for progressive movement are separate from detectors for regressive

2 It is known that the fly's visual system contains movement as well as position detectors though it is still unclear how distinct they are at the physiological level (Reichardt and Poggio, 1981). In order to simplify matters here we refer to movement and position detectors combined to asymmetric detectors. The distinction between position and asymmetric movement detectors is essentially irrelevant for the model described here since they would be combined anyway in a single channel to form the input to the circuitry we propose

movement. Large field pool cells (S_L and S_R) summate the signals from the elementary movement detectors over a large part of the visual field of the two compound eyes and receive a corresponding contralateral input. They inhibit through shunting inhibition the signals provided by the individual detectors, irrespectively of their preferred direction. After shunting inhibition of each channel all signals are summated by other large field output cells (X_L and X_R). Before summation, each synaptic input to the (X_L and X_R) cells undergoes a nonlinear transformation – like a squaring operation – representing either the nonlinear presynaptic-postsynaptic characteristic at the synapse or local active properties of the postsynaptic membrane. It is further assumed that the behavioural response is given by adding to the output of the cells X_L and X_R their running time integral.

Let us now have a closer look at the circuitry's specific operations. The movement detectors for progressive (front to back) motion respond like the movement detectors for regressive (back to front) motion, except that the progressive channels have a higher amplification than the regressive ones (asymmetric). Behavioural experiments indicate that the gain ratio of progressive to regressive channels is about 3 to 1 (Reichardt, 1973; Wehrhahn, 1981). If we designate with N the number of stimulated movement detectors and with x_i the amplitude of the i^{th} detector output, the X_L and X_R cells should respond proportional to $\sum_{i=1}^{N} x_i^n$, where n is the exponent of the last synaptic step which links the detector outputs with the cells X_L and X_R. The pool cells S_L and S_R summate the detector outputs so that we have in the pool a signal proportional to $\sum_{i=1}^{N} x_i$. Each elementary channel is shunted by the pool via presynaptic inhibition. The synapses involved in the process of shunting inhibition should therefore inhibit the output terminal of each elementary detector by opening ionic channels with an equilibrium battery close to the resting potential. If we designate with β the coefficient of shunting inhibition, the operation is described by the expression

$$1 \Big/ \left(\beta + \sum_{i=1}^{N} x_i\right). \tag{2}$$

It is clear then that the output of the cells X_L and X_R is inversely proportional to $\left(\beta + \sum_{i=1}^{N} x_i\right)^n$, where n is again the exponent characterizing the last synaptic transmission. The neurophysiological basis of shunting inhibition and the nonlinear synaptic transmission are considered in Appendix A. To simplify the argument let us assume that the N channels are stimulated in exactly the same way so that all x_i are equal. Under this assumption the output of the cells X_L and X_R would be given by the expression $y = \frac{Nx^n}{(\beta + Nx)^n}$. The last expression does not fulfill the constraint of the specific gain control on N, as y, with increasing N, does not become independent of N. If we assume, however, that the output of the pool saturates so that Nx is replaced by $(Nx)^q$ with $q<1$, the output of the cells X_L and X_R are described by the relation.

$$y = \frac{Nx^n}{(\beta + (Nx)^q)^n} \tag{3}$$

an expression which is discussed in detail in the first part of Appendix B. The output signal y becomes clearly independent of N for large N, if $q = 1/n$. In other words the parameters q and n are coupled in order to fulfill the specific constraint of gain control on N. For $(Nx)^{1/n} \gg \beta$, y approaches x^{n-1}. Since optomotor responses to sinusoidally oscillating patterns are in first approximation sinusoidal, n is restricted to the value $n=2$, so that only one free parameter, the shunting inhibition coefficient β, has still to be determined. The last step in the diagram of Fig. 9a is the transformation on the X cell output by adding to it a running average (T) in its signal path, leading to the DC shift responses to relative motion.

The insets in Fig. 9a indicate the signals present before and at the different levels of the network when figure and ground are oscillated under the conditions discussed in connection with Fig. 3a. The top level of the insets refer to the positions of the oscillating ground and the oscillating figure when the figure is placed in front of the right eye and oscillated with 90° phase shift relative to the ground. At the level of the input channels one period of the signals in the detector channels is plotted. The upper inset on the left side represents one cycle of the ground's movement, whereas the two upper insets on the right side indicate one cycle of the ground's and the figure's movement (at 90° phase shift). The lower inset on the left side represents the summated signals of all channels of the left eye which receive their inputs from the ground. Correspondingly, the respective two insets on the right side represent the summated signals of all channels of the right eye which receive their inputs from the ground (left) and their inputs from the figure oscillating at 90° relative phase shift (right). At the next lower level the signals in the coupled pool cells (S) are plotted (again for one period), namely the contributions from the ground and from the figure. As compared to the input channels, the signals in the pool cells are reduced in amplitude in order to demonstrate the gain of the input synapses and the effect of nonlinear saturation. The

signals at the level of the X_L, X_R cells, that is after the operation of shunting inhibition, are shown in the next lower inset. The last inset shows the signal which is assumed to control the motor output. It is lifted upward (the zero level is located near the bottom of the inset), reflecting the influence of the running average indicated by the T-box. The T-box computes the running integral of the signal $\int_t^{+T} x(\tau)d\tau$ over a time which from our experimental data was chosen to be around $T=400$ ms. This integrated signal is then added to the signal itself with an appropriate weight chosen on the basis of the behavioural data which is the same in all our simulations.

Another neural circuitry that is satisfying the constraints is shown in Fig. 9b. This system is a circuitry with *recurrent* shunting inhibition operating on the individual channels prior to summation of the channel signals in the pool cells (S_L, S_R). In Appendix B it is shown that the associated discrete recurrent system may become unstable, leading to a limit cycle of period 2. If, however, the system is stable, its operation is given by the expression

$$R=Ny^n \quad \text{with} \quad y=\frac{x}{\beta+(Ny)^q} \tag{4}$$

The response R becomes independent of N for large N if the condition $q(n-1)=1$ is fulfilled, whereas in the forward case n and q are coupled by the relation $n\cdot q=1$. The two models lead to $R\approx x$ for large $N\cdot x$ or large $N\cdot y$ if $n=2$, $q=0.5$ or $n=2$, $q=1$, respectively. Interestingly the two circuitries generate practically the same behaviour, their operations however are mathematically different – as pointed out in Appendix B. It seems therefore very difficult to decide on purely behavioural grounds whether one or the other circuitry is realized in the fly's visual system.

It should be added here that the two circuitries are in a sense representing more the logical organisations than the actual neuronal networks. Pool cells (S_L, S_R) and output cells (X_L, X_R), for instance, could consist of interconnected groups of neurons, and must correspond, in any case, to several cells.

5. Comparisons Between Predictions of the Theory and Figure-Ground-Experiments

We shall now test the theory by computing responses to various figure-ground situations. As the two theories lead to practically the same responses, we confine ourselves here to the computations based on the theory for forward shunting inhibition. First, we simulate those situations which led to the experimental results presented in Chap. 3 and second we turn to other situations and compare the computed predictions with the corresponding experiments.

The computer tests were carried out with the following settings: The number of stimulated movement detector channels amounted to 60. Normally we reserved 8 channels for the figure and 52 channels for the ground information. It should be added that the responses do not depend critically on the number of stimulated detectors because of the specific gain control mechanism mentioned before. The free parameter, the shunting inhibition coefficient β, was specified in such a way that the computer results fit the experimental data as well as possible. The parameter settings are $\beta=0.05$, $n=2$, which consequently sets q to 1/2. The integration time for the running average amounted to 0.4 s.

5.1. Simulations of Binocular Experiments

Figure 10a represents the computations of a binocular experiment with relative phase 0° of figure and ground that switches to 90° at time 0.4 s. The response at phase 0° is a sinusoid that changes drastically when the phase changes. Since the running average time amounts to 0.4 s the transition phase ends at 0.8 s. From 0.8 s on the response is stationary, quite similar to the torque response plotted in Fig. 3a. A rising phase is followed by a plateau, a peak and a declining phase. The time average of the stationary part of the response is clearly positive. The "computer fly" is attracted by the figure when oscillating with 90° phase relative to the ground's oscillation.

Quite similar is the result of the computations when the phase between figure and ground oscillations amounts to 270°; all other conditions and parameters remain unchanged. The computer plot is presented in Fig. 10b and should be compared with the corresponding experimental result shown in Fig. 3b. The figure-ground phase shifts from 0° to 270° at 0.4 s. The response reaches a stationary state at 0.8 s. As in the corresponding experiment reported in Fig. 3b, the response phases are now inverted: A response peak is followed by a plateau which is followed by a declining phase. The fly is attracted by the oscillating figure. Time averages of the stationary responses in both computations to figure-ground phases of 270° and 90° lead to the same average attraction value, quite in accordance with the experiments in Fig. 3a and b and with earlier experiments where the time averages of the responses were taken (see Fig. 2).

The next computer simulation tests the figure-ground discrimination at phases 0° and 180°; all other conditions and parameters are as reported before. The result is plotted in Fig. 10c and should be compared with the corresponding experiment in Fig. 3c. The

stationary response after 0.8 s has the same phase (relative to stimulation) as the response to figure-ground phase 0°, whereas the amplitude is slightly smaller. This is in accordance with the experimental test plotted in Fig. 3c where at least no phase change can be observed after the figure-ground oscillation changes from 0° to 180°. The computer simulation leads to a zero time average of the stationary response at 180° figure-ground phase. This is in agreement with the corresponding experiments.

In Fig. 2 we have shown an earlier experiment of a figure-ground test where the time averaged response is plotted as a function of the phase between oscillating figure and oscillating ground. These results as the experimental results reported in Fig. 3a–c are consistent with the computer simulations in Fig. 10a–c that were based on the circuitry presented in Fig. 9a.

5.2. *Simulations of Monocular Experiments*

A surprising result, reported in Fig. 4, is that the figure-ground effect occurs even when the figure oscillates in front of the right eye and the ground only in front of the left eye (contralateral conditions). We have tested this situation in our model and computed the response which is plotted in Fig. 11. Up to 0.4 s, figure and half-ground oscillate in synchrony. The response is oscillatory and strongly negative, due to the fact that the half-ground excites all the photoreceptors of the left eye whereas the 12° wide figure excites a much smaller area on the right eye. The figure-ground phase changes from 0° to 90° at 0.4 s. Due to the integration time for the running average (0.4 s), the new stationary response phase is reached at 0.8 s. The response is of course oscillatory and in the time average positive, relative to the response to synchronous figure-ground motion. The time course of the response at 90° figure-ground phase consists of three regions per period: a plateau, a peak, and a declining phase. The simulation agrees well with the corresponding experiment plotted in Fig. 4.

5.3. *Gain Control Properties of the Model*

In Sect. 3 we have provided experimental evidence for a specific gain control that makes the optomotor response of the fly rather independent from the angular extent of an oscillated texture. We have computed the response to a synchronously oscillating figure-ground environment where the ground's oscillation stops at

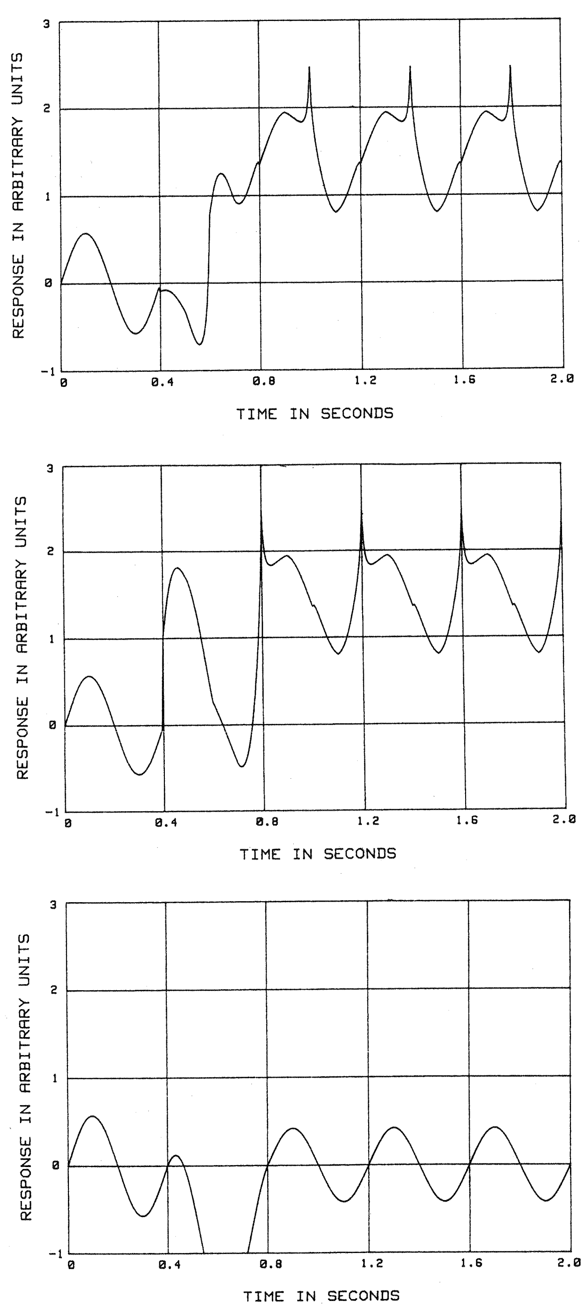

Fig. 10. a Computer simulation of the figure-ground experiment reported in Fig. 3a. Parameters of the simulation are: Number of stimulated detector channels: 60; number of channels stimulated by the ground: 52; number of channels stimulated by the figure: 8; shunting inhibition coefficient $\beta = 0.05$; the exponent n, describing either the nonlinear presynaptic-postsynaptic characteristic at the synapse (linking the detector channels with the cells X_L, X_R) or local active properties of the postsynaptic membrane amounts to $n=2$: q, the exponent describing the saturation of the S_L, S_R cells output, amounts to $q=0.5$; the running average time is one period of response or 0.4 s. The figure-ground phase amounts to $\phi=0°$ and $\phi=90°$. The phase changes from 0° to 90° at 0.4 s. The transition phase is completed at 0.8 s. **b** Computer simulation of the figure-ground experiment reported in Fig. 3b. All parameters and details as described in *a*, except for the relative phase between figure-ground oscillations that amounts here to $\phi=0°$ and $\phi=270°$. **c** Computer simulation of the figure-ground experiment reported in Fig. 3c. All parameters and details as described in **a**, except for the relative phase between figure and ground that amounts here to $\phi=0°$ and $\phi=180°$

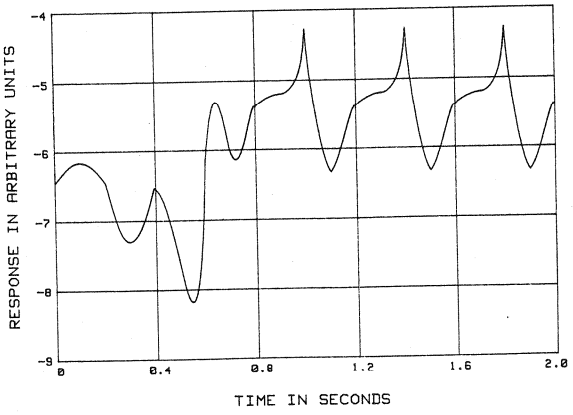

Fig. 11. Computer simulation of the contralateral figure-ground experiment reported in Fig. 4. The oscillating figure in front of the right eye excites 8 channels. The oscillating half ground in front of the left eye excites 30 channels (contralateral condition). The phase between figure and half ground changes from $\phi=0°$ to $\phi=90°$ at 0.4 s and the new stationary state is reached at 0.8 s (due to 0.4 s running average integration time). The response to both phases is negative; less negative however when the figure-ground phase amounts to $\phi=90°$

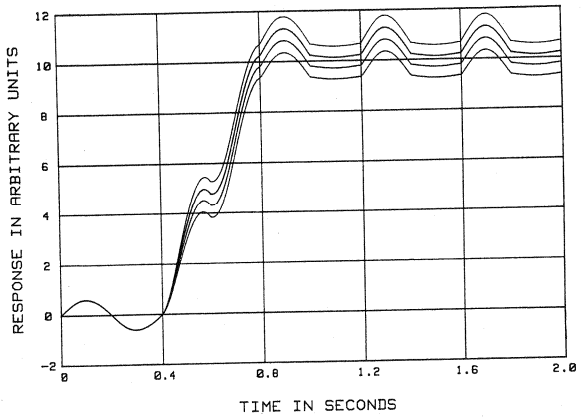

Fig. 12. Computer simulation demonstrating the specific gain control mechanism that operates on the angular extent of the oscillating textured figure. Figure and ground are oscillated in synchrony up to 0.4 s. At time 0.4 s the oscillation of the ground stops whereas the oscillation of the figure continues. Parameter of the stimulation is the angular extent of the figure (1–30 channels). As in the experiments reported in Chap. 3, the "fly" is strongly attracted by the oscillating figure. The attraction increases with an increasing number of stimulated detector channels. However, the effect on the response does not strongly depend on the number of stimulated detectors

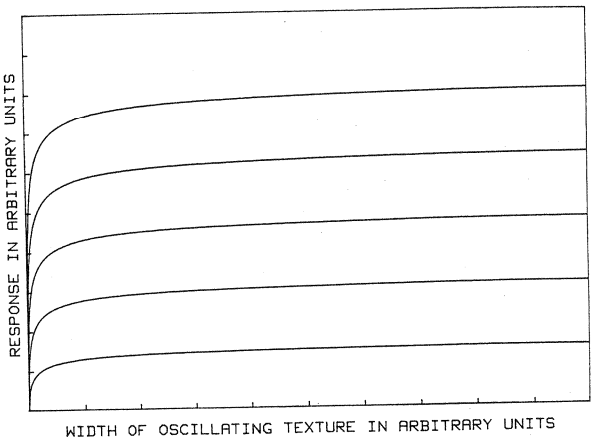

Fig. 13. Computer plot demonstrating the gain control mechanism that operates on the angular extent of the oscillating figure. As pointed out in the text, the model outlined in Fig. 9a relates the detector channel output x to the response y through the relation $y=\frac{Nx^n}{(\beta+(Nx)^q)^n}$. N is the number of excited detectors; n the exponent describing the nonlinear property of the synaptic links between detector channels and cells X_L, X_R and q the exponent describing the saturation of the pool cells S_L, S_R. In the simulations the settings are $n=2.0$ and $q=0.5$; $\beta=0.05$. The diagram shows the response as function of N with x the parameter. The different curves represent different x (from $x=1$ to $x=5$) values. With increasing x, the level of the response plateau increases

0.4 s and only the figure continues to oscillate. The parameter explored in the computer simulation (see Fig. 12) is the angular extent of the figure. The stationary response is positive as in the experiments of Figs. 6 and 8: the fly is attracted by the oscillating figure. The lowest response curve (in the stationary response region) in Fig. 12 refers to a figure stimulating just one channel. The next higher response refers to 2, the next to 15 and the highest response curve to a figure width of 30 channels. Changes in the angular width of the figure have very little influence on the strength of the response – in accordance with our findings in Sect. 3.

Another way of testing the specific gain control is to compute the oscillation amplitude of the response as a function of the figure's width. Parameter of the simulation is the signal amplitude at the detector channel outputs. The result of this calculation is given in Fig. 13. The response increases with an increase of the figure's angular extent and reaches a constant level. However, it strongly depends on the detector channel output. With increasing output, i.e. with increasing oscillation amplitude of the figure, one gets response curves of different levels. The computer simulation is quite in accordance with the experimental data plotted in Figs. 6 and 7; it specifically simulates the experiments plotted in Fig. 7.

The simulations reported here so far dealt with experiments reported in Chap. 3. In the following we will test the circuitry model (see Fig. 9a) with additional figure-ground experiments.

In Fig. 4 we have shown the result of a contralateral figure-ground experiment; therefore it seemed reasonable to test the flies also under ipsilateral conditions, when figure and ground are stimulating only the right compound eye whereas the left com-

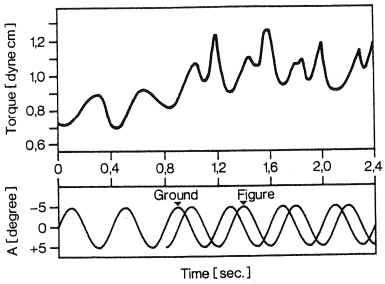

Fig. 14. An ipsilateral figure-ground experiment. All parameters and settings as described in the legend of Fig. 4, except that the textured half ground extends from $\psi = 0°$ to $\psi = +180°$. It therefore stimulates, together with the oscillating figure, the right compound eye only. The response of the fly is oscillatory and increases when the phase of the oscillating figure and ground changes from 0° to 90°. The average response level is positive since only the right compound eye is stimulated during the test. The plot is a 100 sweep average

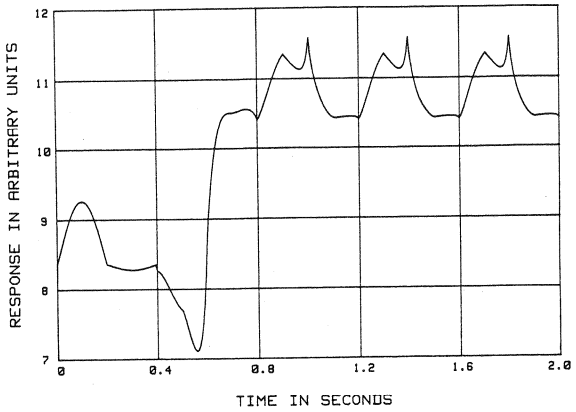

Fig. 15. Computer simulation of the ipsilateral figure-ground experiment shown in Fig. 14. The oscillating figure, in front of the right eye, excites 8 channels. The oscillating half-ground in front of the right eye excites 22 channels (ipsilateral condition). The phase of the oscillating figure changes from $\phi = 0°$ to $\phi = 90°$ at time 0.4 s. The response to both phases is positive: more positive, however, when the figure-ground phase amounts to $\phi = 90°$

pound eye is illuminated but receives no contrast inputs. Otherwise the parameters of the experiment were the same as described in connection with Fig. 4. The experimental result is shown in Fig. 14. For phase 0° conditions (up to 0.8 s) the torque response of the test fly oscillates around a positive value, namely the fly is attracted by the oscillating half ground (since figure and ground stimulate only the right eye). After the phase changes from 0° to 90° at time 0.8 s, the response increases further, leading to an oscillatory phenomenon with apparently two response peaks per period of oscillation. The corresponding simulation is presented in Fig. 15. The zero phase changes at 0.4 s to 90° phase, leading, as in the experiment, to an increase of the response and an oscillatory phenomenon with two peaks in each period.

5.4. *Further Tests of the Model*

In an earlier paper we have also investigated the time average of the fly's response under bilateral ground conditions with a figure oscillating in front of the right eye but with twice the amplitude as the ground. The time averaged responses as a function of the figure-ground phase are shown in Fig. 16. The response is positive (the fly is attracted by the oscillating figure) even when figure and ground oscillate in synchrony since under these conditions there is relative motion between figure and ground. The corresponding simulations, shown in Fig. 17a–d, consist of four computer tests, namely for the phases 0°, 90°, 180°, and 270°. A numerical evaluation of the computer responses show that the time averages for phase 0° and 180° are the same and positive, whereas the time averages for phase 90° and 270° are also equal but larger than for phase 0° and 180°, in agreement with the experimental data shown in Fig. 16.

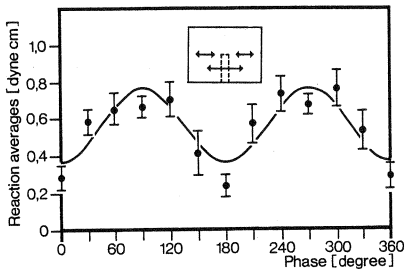

Fig. 16. Phase dependence of the figur-ground discrimination effect. Experimental conditions as described in the legend of Fig. 2, except for different oscillation amplitudes ($\pm 2.5°$ for the ground and $\pm 5°$ for the stripe). Note that the fly is attracted by the oscillating stripe (3° wide) even at phases $\phi = 0°$ and $\phi = 180°$. Each point is an average from 10 flies. (From Reichardt and Poggio, 1979)

In another set of earlier experiments (Reichardt and Poggio, 1979) we had tested the fly's average response when the relative amplitudes of ground and figure oscillations were varied. Parameter of the experiments is the relative phase between figure and ground (either to 0° or 180°). The outcome of these experiments is shown in Fig. 18. The positive response to oscillations of the figure alone is used as a reference value (set here equal to 1). With an increasing ground amplitude the response diminishes and is zero when figure and ground amplitudes are equal. When the ground amplitude increases further the fly's response becomes negative; the fly is then repelled by the figure ("escape response"). At large amplitudes a number of factors reduce the effect. Higher harmonics now become significant. Dynamic saturation at the level of the motor output affects the mean output because of the strong, direction-sensitive, optomotor response. The

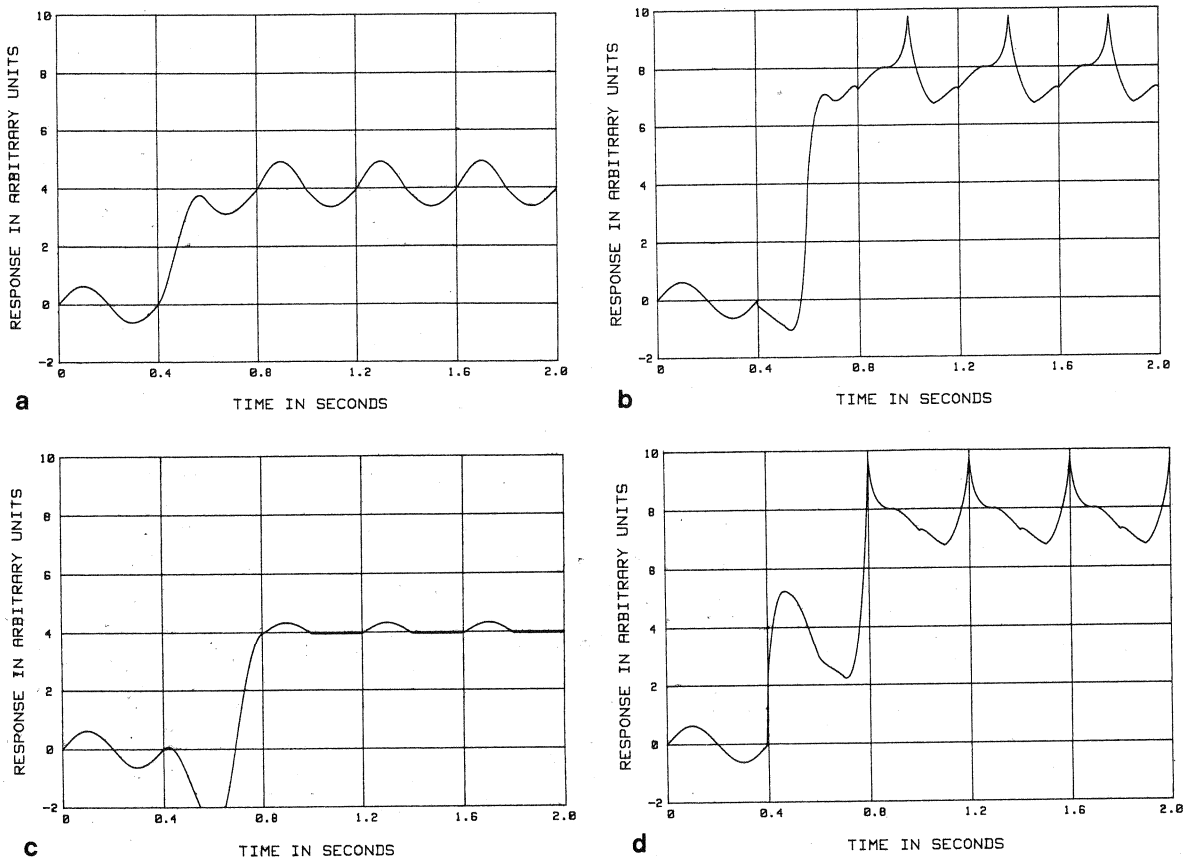

Fig. 17a–d. Computer simulation of the response to a figure-ground test with a figure oscillation amplitude of twice the ground's oscillation amplitude. **a** The amplitude of the oscillating figure changes at 0.4 s; the phase amounts to $\phi = 0°$ throughout the test. **b** The amplitude of the oscillating figure changes at time 0.4 s; the phase changes from $\phi = 0°$ to $\phi = 90°$ at 0.4 s. **c** The amplitude of the oscillating figure changes at time 0.4 s; the phase changes from $\phi = 0°$ to $\phi = 180°$ at 0.4 s. **d** The amplitude of the oscillating figure changes at time 0.4 s; the phase changes from $\phi = 0°$ to $\phi = 270°$ at 0.4 s. More details see text

phenomenon reported here is the same, irrespectively of whether the phase is 0° or 180°. This behaviour is also reflected in the simulations presented in Fig. 19a and b. In Fig. 19a and b the amplitude of the ground switches at 0.4 s to twice the amplitude of the oscillating figure. The relative phase does not change in Fig. 19a whereas in Fig. 19b it changes to 180° at 0.4 s. The simulations show that the average response becomes negative when the ground's amplitude has increased. They are numerically equal when a time average is taken. This is again perfectly in accordance with the experiments reported in Fig. 18.

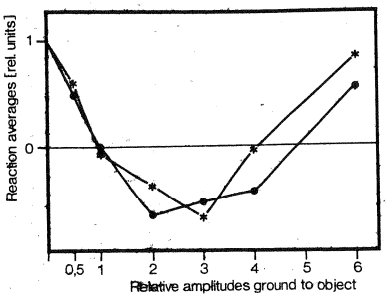

Fig. 18. Torque response as a function of the relative oscillation amplitude of ground and figure. Experimental details as described in the legend of Fig. 2, except for the various oscillation amplitudes of the background with respect to the stripe's unity oscillation amplitude of ±1°. The relative phase relations between stripe and background are: 0° (●), 180° (*). The average standard error of the means is ±0.1 relative units. Each point is an average from 10 flies

So far we dealt with stimulus conditions where the ground consisted of either a 360° or a 180° texture. In the following experiment the ground was replaced by a textured figure of 12° width, positioned at $\psi = -40°$, whereas another textured figure of equal width was mounted at the contralateral position $\psi = +40°$. The two figures were oscillated in two different phase conditions: In synchrony (phase 0°) up to 0.4 s, when the figure in front of the right compound eye was switched to 90° phase relative to the figure in front of the left compound eye. The response of a typical test-fly is shown in Fig. 20. After the initial transients in the response have decayed, the reaction is periodic, with

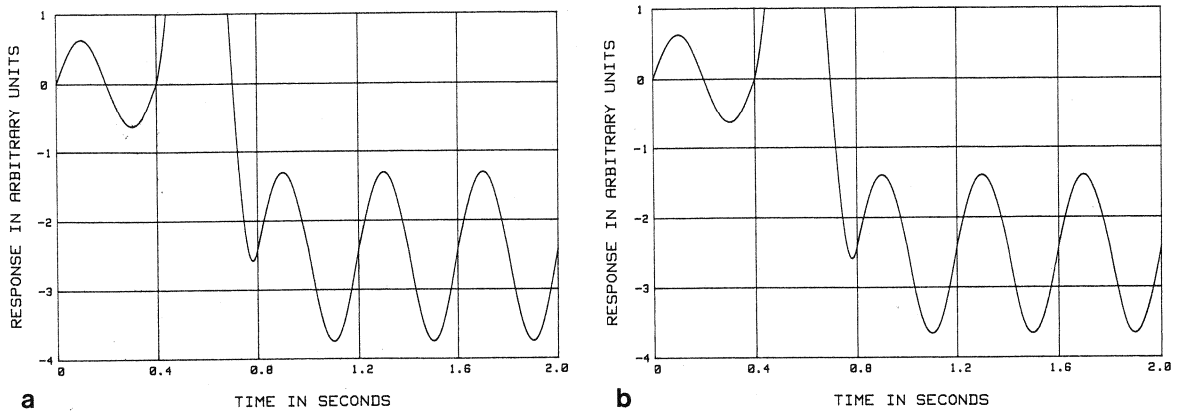

Fig. 19a and b. Computer simulation of the situation described in Fig. 18. **a** The amplitude of the ground's oscillation is doubled at time 0.4 s. The phase remains at $\phi = 0°$ throughout the test. **b** The amplitude of the ground's oscillation is doubled at time 0.4 s. The phase changes at 0.4 s from $\phi = 0°$ to $\phi = 180°$. More details see text

different rising and falling phases. The rising phase has a shallow saddle whereas the falling phase is nearly straight. The amplitude of the response during phase 90° conditions amounts to about twice the amplitude during synchronous oscillation. The corresponding simulation, presented in Fig. 21, is quite in accordance with the experimental tests, indicating that the theory also explains this unusual stimulus condition.

The experiment and computer simulation described before can be used to test the coupling between the two pool cells S_L and S_R in the model of Fig. 9a. In all simulations, discussed so far, the pool cells were coupled (the coupling coefficient amounted to 1). When the coupling is switched off, so that the two cells S_L and S_R operate independently, the corresponding computer simulation leads to about equal response

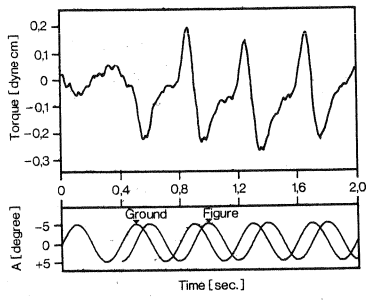

Fig. 20. A bilateral figure-"ground" experiment. A textured stripe of 12° angular width is sinusoidally oscillated in front of the right eye around the mean position $\psi = +40°$. Another textured stripe of the same width is oscillated in front of the left eye around the mean position $\psi = -40°$. Oscillation amplitudes amount to $\pm 5°$. Oscillation frequencies amount to 2.5 Hz. At time 0.4 s the relative phase between Figs. 1 and 2 switches from 0° to 90°. The fly's response is oscillatory around zero torque and increases in amplitude after the phase has shifted from 0° to 90°. At 90° phase condition, the up-response (from negative to positive torque values) contains a slight saddle. Note that the response oscillates around zero. The response plotted is an average of 100 sweeps

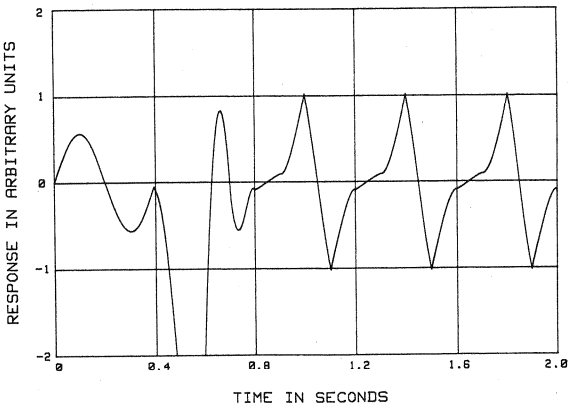

Fig. 21. Computer simulation of the experiment reported in Fig. 20. The number of stimulated channels on both sides are 8. The phase between the oscillations of the two figures changes from 0° to 90° at time 0.4 s. The transition phase is completed at 0.8 s. The similarity between the experimental data and the computed response is striking

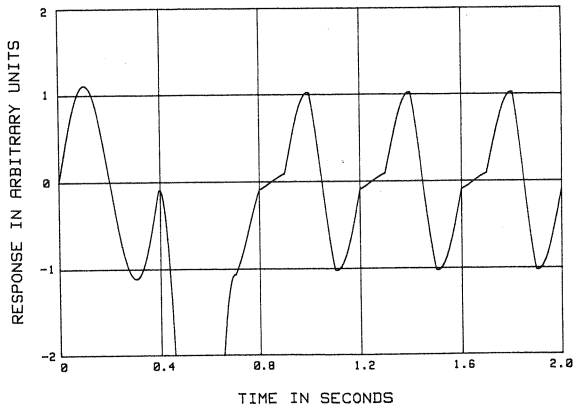

Fig. 22. All details as described in the legend of Fig. 21, except for the decoupling of the two pool cells (S_L, S_R) in Fig. 9a. The main consequence of the decoupling is an increase of the amplitude of the response at phase 0° to a level comparable with the amplitude at phase 90°. This is in contradiction with the experimental finding reported in Fig. 21. For more details see text

amplitudes during 0° and 90° phase conditions, as shown in Fig. 22. This result is a strong hint in favour of a complete pool coupling.

6. Behavioural and Electrophysiological Experiments with the Blowfly Calliphora

One of the main questions arising from the last chapters concerns the actual neuronal realization of the proposed model in the visual system of the fly. Recent electrophysiological and neuroanatomical studies have demonstrated that the main motion areas in the visual system of the fly are located in one of the highest order visual neuropils of each optic lobe. The neuropils are termed lobula plates and contain different classes of large tangential cells, all of which respond selectively to either horizontal or vertical motions. The lobula plates are assumed to be functionally involved in the control of the well known optomotor responses (for review see Hausen, 1981).

The major output cells of each lobula plate responding to horizontal motion are a group of giant neurons called horizontal system (Piernatoni, 1976). It has been shown, that the horizontal system (HS) is specifically involved in the control of the optomotor yaw torque responses (Hausen and Wehrhahn, 1983). In order to investigate whether it is also involved in the neural control of the figure-ground discrimination behaviour, its signals were recorded electrophysiologically under basically the same stimulus conditions as used in the behavioural experiments. For technical reasons, these electrophysiological experiments could not be performed with houseflies but only with blowflies of the species *Calliphora erythrocephala*. Hence, the behavioural responses of blowflies to stimulation with relative motion had to be evaluated in a first series of experiments. The results of these experiments are described in the next two sections of this chapter, followed by a presentation of the electrophysiological findings and a discussion of the data in terms of the proposed model circuitry.

6.1. Time Averaged Behavioural Responses to Relative Motion Stimuli

In these experiments, the time averaged yaw torque responses of *Calliphora* to relative motion are determined as a function of the relative phase between figure and ground. The stimulus setup is identical to that described in Chap. 3. The results are plotted in Fig. 23, in which each point represents the mean torque response obtained from measurements with 10 flies under the phase-conditions $\phi = 0°$, 90°, 180°, and 270°. Positive torque responses represent intended turnings of the fly toward the figure and hence indicate

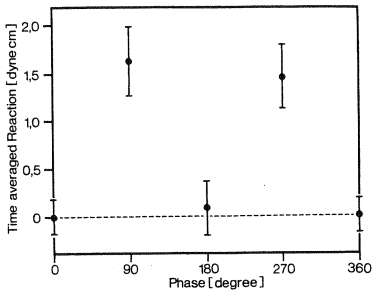

Fig. 23. Time averaged torque responses of *Calliphora* to stimulation with relative motion. The experimental conditions are identical to those described in Fig. 2. Each point represents the response average of 10 flies. Vertical bars denote standard errors of the mean. The response behaviour of *Calliphora* resembles that of *Musca* (Fig. 2): Strong torque responses (towards the figure) are elicited under stimulation with phase $\phi = 90°$ and $\phi = 270°$; at $\phi = 0°$ and $\phi = 180°$ no or only small responses are observed

discrimination of the moving figure from the moving ground. Figure 23 demonstrates clearly that the behaviour of the blowfly under these conditions is essentially the same as that of the housefly (see Fig. 2). The figure is optimally discriminated from the ground for the phase conditions $\phi = 90°$ and $\phi = 270°$. No responses are elicited for phase $\phi = 0°$ and only a very weak response at $\phi = 180°$.

6.2. Dynamics of the Behavioural Responses to Relative Motion

The next series of experiments was carried out in order to determine the instantaneous torque responses of the blowfly in a figure-ground experiment. Again the stimulus conditions are identical to those described in Chap. 3. The results are plotted in Fig. 24 and show the stimulus induced torque responses as a function of time. The recording starts with one period of synchronous movement of figure and ground ($\phi = 0°$). At time 0.4 s, the oscillation of the figure is switched to $\phi = 90°$ as indicated at the bottom of the plot. The recording demonstrates that the torque response of *Calliphora* contains a slow positive component of increasing amplitude under stimulation with phase $\phi = 90°$. This is quite in accordance with the result presented in Fig. 23 and fits well to the behaviour of *Musca* under the same stimulus conditions (see Fig. 3a). In contrast to the latter, however, *Calliphora* does not show the typical signatures in the response dynamics. In particular, the pronounced peaks, found in the responses of *Musca* at $\phi = 90°$ are entirely lacking in the data at our disposal so far. Hence, although the time averaged responses of both species in the figure-ground experiment are highly similar, their response dynamics may show significant differences.

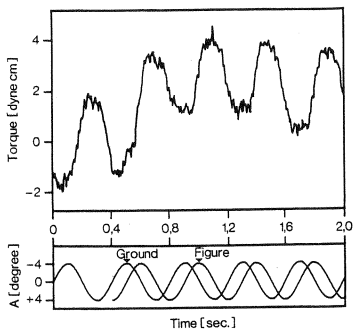

Fig. 24. Dynamics of the torque responses of *Calliphora* during stimulation with relative motion ($\phi = 90°$). The experimental conditions are the same as in the respective experiment with *Musca* (Fig. 3a). The plotted response curve represents the average of 100 sweeps with a typical fly. As demonstrated at the bottom of the plot, figure and ground move synchronously in the beginning and are set to phase $\phi = 90°$ at time 0.4 s. As indicated by the slow positive-going response component starting at time 0.4 s, the fly is attracted by the figure in this phase condition. In contrast to the response behaviour of *Musca*, stimulation with relative motion does not lead to characteristic peaks in the response curve

6.3. Responses of the Horizontal Cells to Relative Motion

Before discussing the electrophysiological figure-ground experiments, the main properties of the horizontal cells shall be briefly summarized. The horizontal system in each lobula plate consists of three giant tangential neurons which are located at the anterior surface of the neuropil and which project to the ventrolateral protocerebrum (Fig. 25). The cells are termed north, equatorial and south horizontal cell

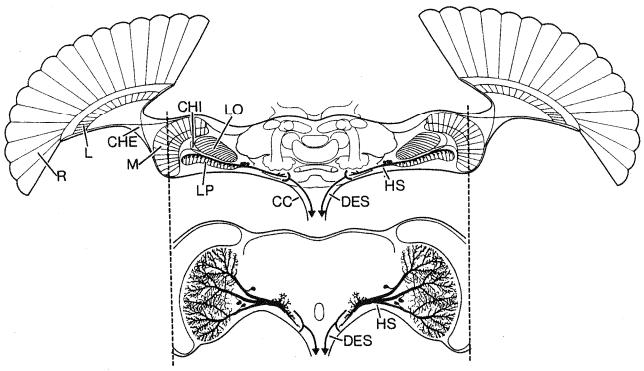

Fig. 25. Schematic horizontal cross-section through the eyes, optic lobes and brain of *Calliphora*. The position of the horizontal system (HS) in the frontal layer of the lobula plate (LP) is indicated. The lower part of the figure shows the horizontal systems of both optic lobes in frontal projection. There is evidence, that the horizontal cells are synaptically linked to descending neurons (DES) which project through the cervical connective (CC) and terminate in the motor control centers of the thoracic ganglion. Recordings were taken from equatorial horizontal cells of right optic lobes. Further abbreviations: CHE: external chiasma, CHI: internal chiasma, L: lamina, Lo: lobula, M: medulla, R: retina

(HSN, HSE, HSS) according to the position of their dendritic fields in the dorsal, equatorial and ventral part of the lobula plate respectively and the corresponding locations of their receptive fields in the visual field of the pertinent compound eye. There is anatomical evidence that the horizontal cells are directly coupled to the motor control centres in the thoracic ganglia via descending neurons, which project through the cervical connective. The horizontal cells are movement sensitive elements which are selectively activated by ipsilateral progressive motion and inhibited by motion in the reverse direction. The response pattern of all three cells to ipsilateral stimulation is basically the same. Although the input wiring of the horizontal cells is not yet analyzed, we will assume in the following that they are postsynaptic to retinotopic arrays of excitatory small field movement sensitive elements (elementary detectors) responding to progressive motion and to inhibitory elementary detectors responding to regressive movement. Whereas the HSS responds only to ipsilateral stimulation, the HSE and the HSN are additionally activated by regressive motion in the contralateral visual field. In all three horizontal cells, the responses to ipsilateral stimulation are not encoded in regular spike trains, but rather in graded shifts of the membrane potentials: stimulation with progressive (regressive) motion leads to depolarization (hyperpolarization) of the cell membrane. Responses to contralateral stimulation in the HSE, on the other hand, induces regular spike activity (Hausen, 1981, 1982a, b; Eckert, 1981). Since a first series of test experiments had demonstrated that the graded responses of the HSN and HSS under stimulation with relative motion did not differ from those of the HSE, only the latter cell was investigated systematically in the following experiments, since its receptive field was best covered by the stimulus panorama. Stimulus induced responses were evaluated in terms of graded potentials; the spike responses to contralateral stimulation were neglected. A total of 23 HSE were studied in this experimental series all of which were found to exhibit qualitatively the same response patterns.

The typical response of an equatorial horizontal cell of *Calliphora* in the figure-ground experiment is shown in Fig. 26. The stimulus set-up is as described in Chap. 2.2. In each case, figure and ground are initially oscillated in phase. Whereas this synchronous movement is maintained throughout the experiment in Fig. 26a, the phase of the figure is set to $\phi = 90°$, 180°, and 270° at 0.4 s in Fig. 26b–d as indicated at the bottom of the respective recordings. Each recording represents the average graded response obtained from 20 repetitive stimulations. The resting potential of the cell is indicated in each recording by a broken line. Positive deviations from the resting potential indicate

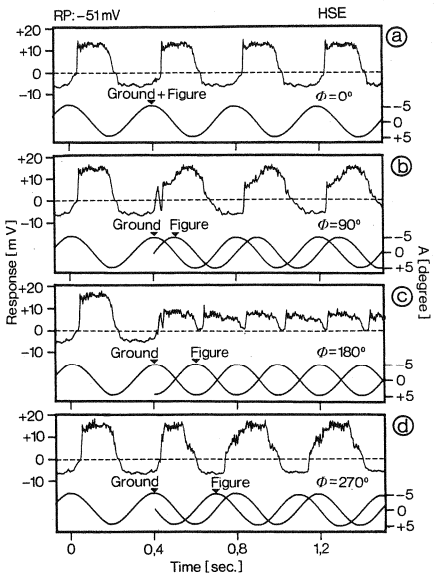

Fig. 26a–d. Instantaneous responses of an equatorial horizontal cell HSE of *Calliphora* to stimulation with relative motion. The stimulus consisted of a binocular ground (subtending $-105° \leqq \psi \leqq +105$) and a 10° wide figure positioned in the right visual field at $\psi = +40°$. Both were oscillated sinusoidally with a frequency of 2.5 Hz and an amplitude of $\pm 5°$. As indicated by the insets, each experiment started with in-phase motion of figure and ground (downward deflection in the stimulus traces denote clockwise motion). At time 0.4 s the phase of the figure was set to 90°, 180°, and 270° as shown in **b–d**, respectively. The recordings were obtained from a HSE of the right optic lobe, having a resting potential of -51 mV (indicated by broken lines). Each recording represents a response average obtained from 20 repetitions of the respective stimulus-sequences. Positive and negative deflections of the measured potentials from the resting potential indicate de- and hyperpolarizing graded responses of the cell. As demonstrated in **a**, the cell is excited by clockwise horizontal motion and inhibited by counterclockwise motion. Under stimulation with relative motion (**b–d**), the instantaneous response of the cell is determined by the superimposed excitatory and inhibitory response components elicited by the clockwise and counterclockwise moving stimulus components

stimulus-induced graded depolarizations and hence activation of the cell. Negative deviations indicate inactivation of the cell.

In case of synchronous figure and ground movement ($\phi = 0°$; Fig. 26a), the HSE responds to the intervals of progressive and regressive motion with graded de- and hyperpolarizations, respectively. It can be clearly seen that progressive lead to larger response amplitudes as compared to regressive motions and that the slope of the recorded response deviates significantly from the sinusoidal velocity profile of the stimulus. These findings are fully consistent with the results of previous studies of the horizontal cells, in which moving periodic patterns were used as optical stimuli. Under stimulation with $\phi = 180°$ (i.e. figure and ground moving in opposite directions; Fig. 26c) we find that exclusively depolarizing responses are elicited in the HSE, and that the amplitudes of the responses are reduced relative to the first experiment with $\phi = 0°$. This is qualitatively to be expected since the stimulus contains now simultaneous progressive and regressive motions which lead to antagonistic responses of the cell. Since the amplitude of the depolarizing response components (to progressive motion of figure and ground) exceeds the amplitudes of the hyperpolarizing response components, a net depolarization of the cell occurs.

The response pattern measured for $\phi = 90°$ and $\phi = 270°$ is somewhat more complicated, but the underlying superimposed de- and hyperpolarizing response components to the simultaneous progressive and regressive movements of figure and ground are still detectable. It should be noted that (a) the time course of the responses to $\phi = 90°$ and $\phi = 270°$ are not significantly different from each other, and that (b) slow positive-going shifts in the membrane potential as well as conspicous peaks comparable to those found in the behavioural data of *Musca* under the same stimulation condition do not occur.

A closer inspection of the recordings reveals an important feature, which is most evident in the experiment with $\phi = 180°$. Under this condition, the effect of the figure-movements on the response of the cell is evidently of comparable size to that of the ground movement. In other words, the cell responds with about equal strength to figure and ground, although the former is much smaller than the latter. The effect becomes even more obvious, when figure and ground are not moved simultaneously, but separately from each other as demonstrated in Fig. 27a and b. Figure 27c shows that the response of the HSE to simultaneous movement of figure and ground is significantly smaller than the sum of the constituent response components. It must then be concluded that the response amplitude depends in a highly nonlinear fashion on the size of the stimulus during both progressive and regressive motion. This is consistent with previous results (Hausen, 1981, 1982b), in which the spatial integration properties of the HSE have been studied in more detail. These experiments demonstrated that under stimulation with large moving patterns, the response amplitudes of the HSE become nearly independent of the stimulus size. It has been shown that the nonlinear response behaviour does neither depend on simple postsynaptic saturation of the cell during stimulation with large patterns nor on direct inhibitory interactions between its excitatory and inhibitory input channels. The effect can be explained, however, by a gain control mechanism as proposed in the present model, in which the individual excitatory (progressive sensitive) input channels are inhibited by large field cells sensitive to progressive motion; the

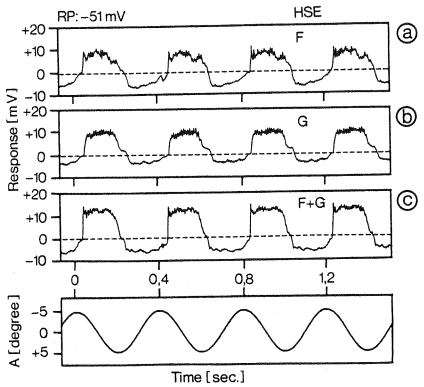

Fig. 27a–c. Instantaneous responses of an equatorial horizontal cell HSE of *Calliphora* to **a** stimulation with a moving figure in front of a stationary ground, **b** to stimulatiion with a moving ground behind a stationary figure, and **c** to synchronous movement of figure and ground. Despite their considerable difference in size, figure and ground are about equally effective with respect to the amplitudes of the elicited responses in the cell. The response obtained in **c** is significantly smaller than the sum of the responses obtained in **a** and **b**. This response behaviour indicates inhibitory interactions in the input wiring of the HSE. Stimulus parameters and recording condition as specified in Fig. 26

inhibitory inputs should be inhibited by regressively sensitive large field cells.

6.4. How Does the Model-Circuitry Fit the Electrophysiological and Behavioral Data Obtained from Calliphora?

The model for figure and ground discrimination as proposed in Chap. 4 relies on nonlinear inhibitory interactions between large field movement sensitive elements and arrays of directionally selective elementary movement detectors. The signals of the latter are modulated by this interaction and are subsequently integrated by large output elements which determine the behavioural response of the animal. When comparing the response of the horizontal cells of the lobula plate and those of the output cells X_L and X_R of the model during stimulation with relative motion one finds several striking similarities:

(a) Both cells are directionally selective movement sensitive large field elements.

(b) Both cells are excited by progressive motion in the ipsilateral visual field and are inhibited by regressive motion; in both cases progressive motion elicits stronger responses than regressive motion.

(c) The responses of the X-cells of the model reflect the gain control properties of their input-wirings; the HSE seems to underly also a gain control mechanism.

On the basis of these findings it is highly suggestive to consider the horizontal cells of both optic lobes as likely neuronal candidates for the output cells X_L and X_R of the model.

This assumption leads to the question of whether the response dynamics of the model output cells X and the HSE during the figure-ground experiment are compatible. It has been demonstrated above that the behavioural responses of *Musca* and *Calliphora* differ considerably in this respect. It cannot be expected therefore that the computed responses of the cells X as shown in Fig. 10a (which are fitted to the situation in *Musca*) are compatible with the responses of the HSE in *Calliphora* (see Fig. 26). The question arises, is it possible to change the model coefficients in such a way, that both the measured response dynamics of the HSE and the measured torque responses of *Calliphora* can be simulated in a satisfactory manner?

As described in Chap. 3, the signal of the output cells X is given by Eq. (3):

$$y=\frac{Nx^n}{(\beta+(Nx)^q)^n},$$

where x denotes the signals of the N input channels, β is the coefficient of the shunting inhibition, q determines the nonlinear saturation of the pool cells S and n represents the nonlinearity in the signal transmission of the synapses between input channels and the output cells X. In the original model, we have set $q=0.5$ and $n=2$ in order to achieve a satisfactory simulation of the behavioural responses of *Musca*.

It is obvious that the sharp peak-responses obtained in cell X upon stimulation with $\phi=90°$ depends strongly on the value of n (q kept at 0.5). Thus, reduction of n results in a reduction of the peak amplitudes and finally abolishes them. The latter is the situation found in the responses of the horizontal cells of *Calliphora* and can be approximated with the model by setting $n=1$ which means that the synapses of the single motion detector channels on the output cells X are now assumed to have a linear input-output-characteristic. The response of the *Calliphora* HSE and the model output cell X computed with this value of n is shown in the upper curves of Fig. 28 for one period of relative motion with $\phi=90°$.

If we now compare the behavioural output of the model with the actual behavioural responses measured in *Calliphora*, (lower curves in Fig. 28) we find them also in satisfactory agreement. The slow, positive-going reaction component measured in the behavioural experiments at $\phi=90°$ and $\phi=270°$ (see Figs. 23 and 24) is lacking in the simulation and can be generated – according to the original *Musca*-model – by introducing a running average routine in the channel between the output cells X and the site of torque generation.

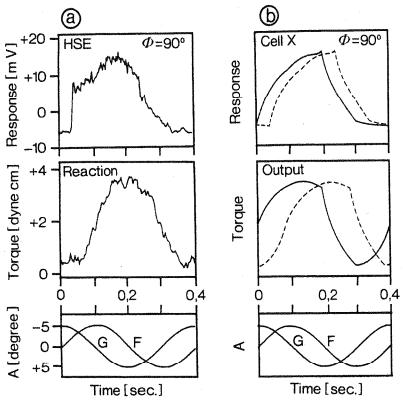

Fig. 28a and b. Response of an equatorial horizontal cell HSE and torque response of *Calliphora* to one period of relative motion at phase $\phi = 90°$ (**a**) as compared to the simulated response of the model output cell X_R and the "behavioural output" of the model (**b**). The relative motions of figure and ground are indicated in the insets. The data in **a** were taken from Figs. 24 and 26b. Both the response of the HSE and the behavioural response show certain delays with respect to the stimulation, which are due to synaptic delays and transmission times in the nervous system of the fly. For better comparison, the simulations (solid lines in **b**) are shown also with respective delays (broken lines in **b**). See text for further explanation

In summary then, we can simulate the behavioural responses of *Musca* on the one hand, as well as the behavioural responses and the responses of the HSE in *Calliphora* on the other hand with the same model circuitry. On the basis of these results it is tempting to assume that the horizontal cells of the lobula plate are indeed the neuronal equivalents of the model output cells X. This inference must be treated, however, with caution since two major problems regarding their input circuitry are unsolved:

(a) there is no evidence, that the progressive and regressive sensitive input channels to the horizontal system are mutually inhibited during ipsilateral stimulation with simultaneous horizontal motion in both directions and also during contralateral stimulation as assumed in the model;

(b) the horizontal cells (HSE and HSN) receive direct excitatory input from a contralateral cell sensitive to regressive motion which is not in accordance with the model circuitry. Hence, although the horizontal cells, as major output cells of the optic lobe controlling yaw torque, show response properties similar to the model output cells X, definite statements about their role in figure-ground discrimination will only be possible after further investigations. For instance, it cannot be excluded that the neuronal implementation of the model circuitry contains two subsystems both contributing to the behavioural response; the horizontal system would then represent the output of only one of them (see Discussion).

7. Discussion

7.1. Structure of the Discussion

This article is about an important aspect of the analysis of motion by the visual system of the fly, the detection of relative motion between an object and its background. Its main goal is to propose a specific neuronal circuitry for this task and to compare its theoretical performance with behavioural and physiological experiments. The main problems to be discussed here fall therefore under two broad categories: neuronal implementation of the model circuitry and functional role and properties of the object-surround computation.

7.2. Neuronal Circuitry

7.2.1. Do the Model Elements Correspond to Real Cells?

The neuronal circuitry shown in Fig. 9a and simulated in our computer experiments is nothing more than the bare skeleton of an actual piece of nervous system. Although the main components of the model – like the pool cells (S) and output cells (X) – are indeed physiologically plausible, several neurons are likely to correspond in reality to each model cell and many connections to our signal paths even if our proposal is basically correct. For simplicity the model contains only one pool cell and only one output cell for each eye. In strict terms this is clearly unrealistic: figure-ground detection is probably performed in each part of the full visual field (Reichardt and Poggio, 1979, Figs. 8, 9, and 19) and we expect that several large field cells would cover this whole range. This is certainly the case for the horizontal system – a possible correlate of the output cell (X) of the model – consisting of several giant neurons, each with a receptive field covering a different part of the visual field of the eye along its dorso-ventral axis. One or several pool cells, probably interconnected, could be associated with several output cells; their binocular connections may be rather complex. There are additional factors that suggest a much more complex circuitry. The model – and all our experiments – only consider the control by horizontal motion of one degree of freedom in flight, i.e. the optomotor yaw torque. The horizontal system seems indeed involved in the generation of torque (Hausen and Wehrhahn, 1983). Additional cells – controlling for instance pitch, roll, lift, and thrust – are certainly also existent (Hausen, 1981). Again, these additional systems may be interconnected to some extent with the circuitry responsible for yaw torque control. Furthermore, the yaw torque response depends on motions which are not restricted to the horizontal direction around the fly. Detection is evident in the fly's torque when the object and the surround move one vertically and the other horizontally and vice versa

(Reichardt and Poggio, 1979). To account for this and similar properties, the circuitry needs to be somewhat more complicated (although preliminary work indicates that minor changes can account for old and new data on horizontal-vertical object-surround separation). The conclusion is thus inescapable that the actual circuitry is richer in cells and connections than the skeleton circuitry analyzed here. Its scope is mainly to bring into sharp focus the essential features of our proposal and to submit them to critical experimental tests. Duplication of cells and increased complication of the actual neuronal circuitry, as found by physiological experiments, may still be functionally equivalent to the basic circuitry skeleton that we propose. An especially interesting "replication" of the circuitry deserves however a special mention. We turn now to this point.

7.2.2. One or Two Systems? The gain control and object specificity of the circuit of Fig. 9a depend on the value n in a sensitive and interesting way. For n smaller than 2 (the value we have assumed in this paper), the sharp peak (at 90° or 270° phase shift) decreases and finally disappears as in the *Calliphora* simulation (see Fig. 28). Simultaneously, if other parameters remain unchanged (in particular $q=0.5$), the effectiveness of the gain control also diminishes and the response increases with the size of the pattern. Values of n larger than 2 bring about converse changes in the properties of the model: the peak amplitude at 90° or 270° phase shift becomes much larger than the whole field response. For $n \geqq 4$ the response to whole field stimulation is negligible, whereas small figures elicit a very strong signal by themselves or for relative motion against a surround (Fig. 29). A circuitry with high n would therefore be extremely sensitive to the motion and relative motion of a small object and almost silent for large field motion of a textured surround. From a computational point of view it is certainly attractive to keep separate early on the detection of small moving objects from the optomotor reaction to surround motion, since their goals – fixation and tracking vs. stabilisation of the flight course – are different. For this reason one may expect in the visual ganglia of the fly two or more anatomically distinct circuitries of the type of Fig. 9a with high and low n, respectively. Could then the behavioural response we measure simply represent their mixture? The answer to this question may come from physiological recordings on lobula-complex neurons that are sensitive to small objects (Egelhaaf, in preparation). Interestingly, Collett (1971) and Collett and King (1975) described similar small field units in the privet hawk mooth and in hoverflies which are shut off by surround motion but respond to small moving targets. Two different figure-ground systems were also suggested by the two different relative movement algorithms found in our earlier analysis (Reichardt and Poggio, 1979) for low and high frequencies of oscillation, respectively. Similarities with the two separate inhibitory mechanisms underlying the response of the lobula giant movement detector system of some Orthoptera (Palka, 1969; O'Shea and Fraser-Rowell, 1975) are suggestive but probably quite superficial. Various types of small field cells inhibited by surround motion are likely to exist in the optic lobes of insects. From the circuitry point of view they may be similar to a small visual field analogue of the output cell (X) of the forward model (see Fig. 9a), receiving only a few inputs, possibly with high synaptic gain (n). Their function,

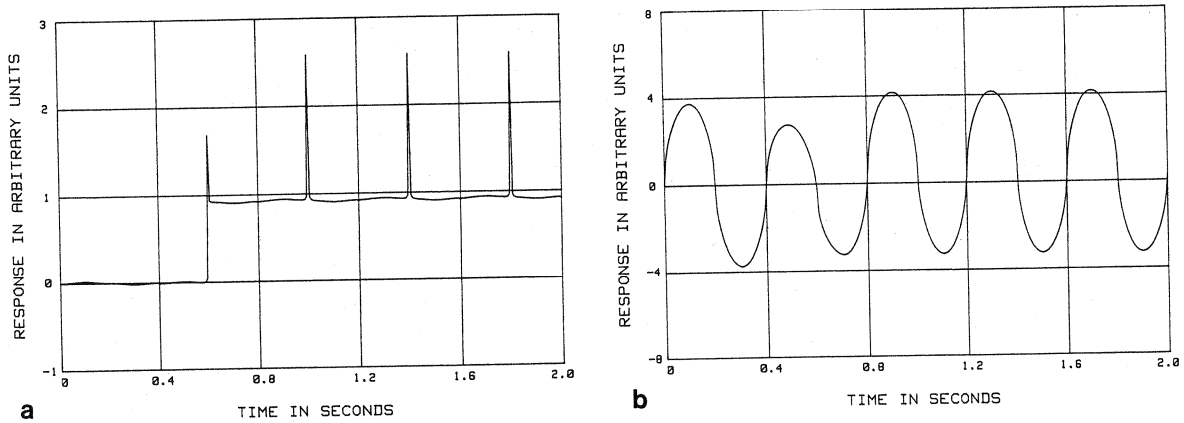

Fig. 29. a Simulation by the forward circuitry with a high synaptic gain ($n=4$). All other parameters are the same as in the rest of the paper. Motion of figure and ground is coherent until time 0.4 s when relative motion starts with a 90° phase shift. The figure is very small, stimulating only one movement channel. The modulation of the response is negligible for whole field stimulation but very strong for (relative) motion of a small object. The output cell is thus very sensitive to small field relative motion and unresponsive to large field motion. **b** Same conditions as in **a** but with low synaptic gain ($n=1$). The output cell now behaves as a unit sensitive to large field motion

however, may be quite different and not directly related to the behaviour analyzed here.

7.2.3. Does the Circuitry Account for Behaviour Variability? When one takes a close look at the response of different individual flies, it is immediately obvious that the figure-ground discrimination behaviour shows a significant variability in the dynamics of the response. The sharp peak characteristic for the 90° or 270° phase situation in *Musca* is an especially sensitive feature of the dynamics: its amplitude may habituate rapidly and is certainly different in different individuals. There is also interspecies variability: the available data on *Calliphora* and *Drosophila* (Bülthoff, 1981) fail to show the sharp Musca-like peaks (at 90° or 270° phase shift). Although behavioural variability and plasticity are in general not surprising, especially in rich sensory environments, it is natural to ask whether our model can easily account for these differences. The answer to this question is indeed positive. As discussed above, the peak depends critically on the parameter n describing the nonlinear transduction at the synapses between the elementary movement detectors and the output cells (X). A plausible biophysical basis for this nonlinear transformation (for an alternative possibility see Poggio et al., 1981), outlined in Appendix A2, is the sigmoidal transformation between presynaptic and postsynaptic potential. Different values of n can arise simply by a shift of the working range of the synapse via a decrease or an increase in the "resting" value of the presynaptic potential (for instance as an effect of multimodal inputs). This is simply one of the several plausible mechanisms but it shows that variability of the peak amplitude in the response is not surprising at all, given the physiological basis assumed in the model.

7.2.4. The Input to the Circuitry. The circuitry proposed in this paper has a retinotopic array of elementary movement detectors as its inputs. The detailed properties of the motion detectors are not critical for the analysis of this paper. In our simulations we have simply assumed that the motion computation was available. Asymmetric multiplication-like elementary motion detectors would be fully satisfactory. Preliminary simulations by Bülthoff (pers. comm.) of the full circuitry – including the computation of movement by such motion detectors – confirm this. A plausible circuitry for motion detection may be based on the synaptic mechanism suggested by Torre and Poggio (1978) and Koch et al. (1982) to explain the direction selective properties of some retinal ganglion cells. If a similar interaction is used by the fly's elementary movement detectors, it is likely to operate on the output of neurons having a receptive field with an excitatory center and horizontally extending inhibitory flanks (Srinivasan and Dvorak, 1980) – a scheme which has several attractive and intriguing properties (Poggio, 1982). The elementary motion detectors need only to be separated in detectors for progressive and regressive movement, respectively, with a different weight. It is irrelevant for our analysis whether inputs from position detectors are also present (they may in part be responsible for the progressive-regressive asymmetry). In a physiological implementation of elementary movement detectors a flicker component may easily arise, at least under some conditions.

7.2.5. Where is the Running Average Performed? In order to account for the shift in the baseline of the response at the outset of relative movement of the figure (for instance at 90°) our model adds to the output of the X-cell its running time integral over a time of about 400 ms. Our computer simulations show that this simple assumption is adequate to account for the available behavioural data. A similar transformation is also performed on the oculomotor signals in primates: a pulse of activity is transformed into the sum of a pulse and its integral before reaching the motoneurons (Carpenter, 1979). It is not difficult to see a possible function of this scheme. The model of Fig. 9a detects an object against a surround only at such instants of time in which sufficient relative motion occurs. At other instances of time the signals corresponding to the object may disappear. This is for instance what happens in the case of 90° phase shift, where "detection" is not uniform over the whole oscillation cycle. It seems therefore reasonable to provide the detection algorithm with some kind of short term memory that can fill-in the short times in which there is no relative motion between a target and the surround. A running average is clearly a very simple way to model this kind of short term memory. It integrates the motor command into a smooth signal and adds it to the high-frequency response of the circuitry. The neuronal realization of this stage will probably be quite different from a pure, linear running average, but we can not at this point advance a more detailed scheme. Interestingly, the transformation of a signal into the sum of the signal itself and its low pass version may be implemented by a positive feedback loop with a low pass filter in the feedback path and an overall equivalent time constant which can be much longer than the filter time constant. Other possibilities of course exist and cannot be excluded. In any case, the data available so far suggest that the operation corresponding to our running average may be located near the motor output, since we do not know of any neuron in the visual ganglia with a response showing a running average component, whereas various kinds of optomotor behaviours – and not only

figure-ground discrimination – contain long time constants.

7.2.6. Is the Circuitry Forward or Recurrent? The inhibition stage in the model is not necessarily of the forward type. The recurrent circuitry of Fig. 9b is a plausible alternative. One of its attractions is that an explicit saturation mechanism in the pool cells is not needed. Its main disadvantage is the potential onset of oscillations (see Appendix B) and even instabilities, especially in a physiological realization of the circuitry where delays in the transmission and transduction of signals cannot be avoided.

Obviously the two schemes are quite different with correspondingly different mathematical descriptions (see Appendix B). Their output properties, however, can be extremely similar for an appropriate choice of the parameters. An input-output type of analysis, like behavioural analysis, is probably helpless for deciding between the two alternatives. In the spirit of our discussion of one or two networks (Sect. 7.2.2) it is even conceivable that both schemes may be actually realized in different neurons.

7.2.7. The Circuitry and Forth-Order Interactions. In earlier papers (see Reichardt and Poggio, 1979) the algorithm used by the fly to detect relative motion was characterized in terms of the corresponding nonlinear interactions between input channels. In the technical language used in those papers the algorithm was described as based on fourth (and possibly higher) order interactions. Our analysis indicated that the computation of relative motion by the fly's visual system requires the inhibitory, multiplication-like interaction of pairs of movement detectors across the visual field. Under the conditions used in this paper (oscillatory frequency 2.5 Hz) the object (figure) detection roughly corresponds to a simple rule: There is an object when there is a significant difference of activity within a retinotopic array of direction sensitive motion detectors, irrespective of their sign.

It is then natural to ask, what is the connection between this algorithmic characterization and the circuitry proposed here? Already a superficial look suggests that the circuitry has indeed the correct properties: it certainly implements the simple rule stated above and it contains multiplication-like interactions between motion detectors, since shunting inhibition is a kind of "dirty" multiplication (see Torre and Poggio, 1978). Thus each movement detector is "multiplied" with the sum of many motion detectors, represented in the pool cell activity. The direction insensitivity of the interaction is directly reflected in the anatomy of the circuitry: both progressive *and* regressive motion inhibits progressive and regressive detectors. All critical properties of the figure-ground detection algorithm – especially from the point of view of time averages – depend on this multiplication-like interaction between motion detectors. Thus our earlier analysis underlines the critical importance of shunting inhibition in the circuitry we propose. Linear inhibition for instance cannot be used. Furthermore, other features of the circuitry, like the saturation of the pool cells and the nonlinearity at the output synapses, though important, are not necessary for performing the computation of relative motion.

The multiplication-like property of the circuitry can also be derived in a more formal way directly from Eq. (3). We sketch very briefly the main steps of the argument. Imagine for simplicity that each detector measures at any given instant either the motion signal x_1 (for the ground) or x_2 (for the figure). Assume furthermore as usual (see Appendix B) that β can be neglected; then the response can be written as

$$R \approx \frac{N_1 x_1^2 + N_2 x_2^2}{N_1 x_1 + N_2 x_2}, \tag{5}$$

where N_1 and N_2 are the number of detectors looking at the ground and at the figure, respectively. For simplicity again assume that $N_1 = N_2$. The output of the circuitry becomes

$$R \approx \frac{x_1^2 + x_2^2}{x_1 + x_2} = x_1 + x_2 - \frac{2x_1 \cdot x_2}{x_1 + x_2} \tag{6}$$

and contains an inhibitory term which is indeed proportional to the product of pairs of motion detectors. The normalization factor $(x_1 + x_2)$ reflects the gain control operation performed by the circuitry and would lead to the additional terms of order higher than four suggested by our earlier analysis (Reichardt and Poggio, 1979; Poggio and Reichardt, 1976).

One more point should be briefly mentioned. In this paper we did not study the figure-ground behaviour at low oscillation frequencies. Previous experiments with time averaged responses showed that the phase dependency of detection changes characteristically when the oscillation frequency is below 1.5 Hz (Reichardt and Poggio, 1979, Fig. 18). We interpreted this finding in terms of a large field motion detector inhibiting small field detectors; this interaction becomes direction selective for low oscillation frequencies. More work is needed to determine the possible correlates of this in terms of our model circuitry. A simple possibility (see also Reichardt and Poggio, 1979) is that the frequency dependence of the behaviour reflects the presence of two different neuronal circuits, perhaps with the different gain control properties and receptive field sizes discussed earlier (see Fig. 24 in Reichardt and Poggio, 1979).

7.3. Computational Properties

7.3.1. What is the Circuitry for? The beginning of a computational analysis of a visual process is the answer to the question, what is it for? The two main properties of the circuitry proposed here are the detection of relative motion and the gain control of the optomotor response to make it independent of pattern size. Which one of the alternatives is the goal of the computation? The answer does not need to be one-sided. Both goals are important for the flight behaviour of a fly. We will discuss later figure-ground discrimination. Independency of the optomotor response from the surround-size – achieved by the gain control mechanism – may have some advantages for stabilizing the course in aerial navigation, independently of the structure and the visible extent of a textured surround, hence of the number of active elementary motion detectors. In addition, it is clearly important that the optomotor response remains sensitive to important stimuli paramcters, like contrast and velocity, since response saturation is avoided by the gain control mechanism. The computation of optical flow and in particular the computation of the correct direction of motion by a system of movement detectors, would necessarily require a gain control property very similar to the one shown by our experiments and by our circuitry. The response should then be independent of the number of stimulated detectors, but depend on the velocity of motion. The hypothesis that the gain control property is a necessary step for the computation of the field of retinal velocities (or at least of their directions) is attractive and intriguing. Several experiments suggest themselves for testing it, some are already in progress in our laboratory.

Thus, though either one of the two main properties may be a side effect of the circuitry, this is highly improbable, given their usefulness and importance. Furthermore, two distinct circuitries, as suggested earlier in this discussion, may indeed coexist, one mainly responsible for the optomotor gain control and the other one for the object surround discrimination.

In any case, there is little doubt that an obvious goal of the information processing performed by the visual system of the fly – and by our model circuitry – is figure-ground separation. Its importance for a fly and for many biological organisms can hardly be underestimated. We now discuss this point.

7.3.2. Uses of Relative Motion (and Texture Differences). The central role of object surround separation in biological visual systems (and computer analysis of time varying imagery) based on motion information alone, is not surprising, given that motion permeates the visual world. Later we will see that also texture differences can be used in a similar way by the neuronal circuitry of Fig. 9. We now ask, what are the specific computational uses of relative motion? It is obvious that relative movement of an object against a background can be used for two tasks: first, to detect its presence and, second, to delineate and localize precisely its boundaries. For tracking and fixation by flies, as well as for early warning in escape responses, precise delineation of object boundaries is not necessary and cannot be revealed by the experiments described in this and our previous papers. Our model circuitry, however, can in principle perform also localization of relative motion discontinuities: The retinotopic array of elementary motion detectors, immediately before the summation by the output cell X, shows the position of the discontinuity boundaries *via* significantly larger local activity. The nonlinear synaptic operation ($n=2$ or larger) enhances this effect; a running average at this stage – i.e. on each single motion detector channel – would maintain the activity boundaries also between short time intervals in which relative motion between an object and surround may disappear because of the irregular motions that take place in the real world (compare the 90° or 270° phase experiment).

The human visual system is capable of both detecting *and* localizing the boundaries between a moving object and the surround on the basis of motion information alone. As pointed out by Hildreth (personal communication), however, our ability to localize the boundaries is different from our ability to detect that relative motion exists in an image. This is clearly expected even in terms of our model circuitry. Furthermore, a difference in speed alone is sufficient to define a relative motion boundary (Richards and Lieberman, 1982). Discrimination also depends on the difference in direction of velocity; for horizontal motion 180° phase shift seems to be almost as detectable as 90° in psychophysical tests (Mac Kay, 1977; personal communication). As one would expect for the fly's case, human psychophysics suggests that a precise computation of retinal velocities is not essential for the detection of motion discontinuities (Hildreth, personal communication). This point bears upon the critical problem which must be first addressed in a computational theory of the figure-ground separation process: on what motion measurements does the computation operate?

7.3.3. Precise Measurements of the Optical Flow are Difficult. In measuring visual motion, one could take a discrete approach and match features between successive temporal frames, similarly to schemes suggested for stereopsis (see for instance Marr and Poggio, 1977; Marr and Ullman, 1981). Alternatively one could take measurements of local fluxes (i.e. func-

tionals of it) from the time dependent light changes provided by the photoreceptors. We consider here only the second of these possibilities: it is the only one used by the fly's visual system, and it plays an important role in the human visual system and in various computer programs for the analysis of time-varying imagery.

As we have stressed several times (see for instance Poggio and Reichardt, 1976, 1981) the motion of an image is not given directly but must be computed from the initial measurements provided by the photoreceptors. Precise computation of the whole optical flow, i.e. the vector field of retinal velocities, has been often assumed in the computer literature, and is critical for schemes that aim to recover three-dimensional shape (Longuet-Higgins and Prazdny, 1980). As computer vision research progressed, the problem of computing the correct velocity field proved to be very difficult (see Marr, 1982). One of the typical problems is that local measurements can only detect the component of velocity perpendicular to the intensity gradient (Fennema and Thompson, 1979; Horn and Schunck, 1981; Marr and Ullman, 1981). A sinusoidal grating – and every 2-D pattern that can be decomposed in such Fourier-components – may move parallel to its edges but there is no local way to detect this movement component. The computation of true retinal velocities requires the combination of various local measurements over an area of the image (see Horn and Schunck, 1981). This usually leads to considerable problems in the computation of the velocity field at object boundaries. In addition, many biological motion detection schemes cannot reliably measure velocity even for one dimensional motions. Their output typically depends on contrast and on a mixture of velocity and spatial structure of the pattern. Algorithms that can be approximated as a second order polynomial functional have this property in an extreme form: their average output depends not on velocity but on contrast frequency, i.e. the ratio, for each spatial Fourier component, of velocity and wavelength. The relative generality of the multiplication-like second order description (see Poggio and Reichardt, 1976; Torre and Poggio, 1978) for biological systems suggests that this may be a rather widespread property of motion detection in biological systems. The optomotor response of flies certainly confounds spatial texture (i.e. wavelength) with velocity and there is good evidence that our subjective evaluation of grating speed has similar properties (when tracking is not allowed; see for instance Diener et al., 1976; Burr, 1982). Although detectors of the multiplication-like type can be made more specific to velocity by preliminary bandpass filtering of the spatial inputs (for instance by center-surround neurons), precise measurements of retinal velocity in terms of these schemes are difficult. But, more importantly, they are not needed for figure-ground separation.

7.3.4. The Coherence Assumption. Simpler motion primitives than precise optical flow measurements are indeed seen to be desirable, when the goal of the object-surround computation and general constraints about the visual world are taken in account. The key observation here is that object boundaries are revealed not only by discontinuities in the velocity field but also by discontinuities in the spatial structure, i.e. in the texture. Thus primitive measurements of motion with the only property that they provide different time varying signals (if either the velocity of the texture changes) fulfill both requirements, which are ultimately based on the physical constraint that matter is cohesive, and is separated into objects. The schemes that have been advanced as elementary motion detectors (Reichardt, 1957; Barlow and Levick, 1965; Poggio and Reichardt, 1973, 1976, 1981; Torre and Poggio, 1978; Koch et al., 1982; but see Marr and Ullman, 1981) all have this property. With an array of such time dependent measurements as the input representation, the figure-ground computation becomes equivalent to detection and localization of incoherence boundaries between those time signals. This is exactly the operation implemented by the circuitry we proposed with multiplication-like detectors as its inputs (see also Reichardt and Poggio, 1979). The circuitry will detect a black-white bar against a random dot pattern of the same contrast, even in the absence of relative motion, because of the different texture (but only for large enough motion amplitudes). Behavioural experiments show clearly that flies will also detect and attempt to fixate this bar for rigid motion of object and surround. Other preliminary experiments indicate that differences in spatial structure (for instance wavelength of a grating) can be artificially camouflaged by appropriate differences in oscillation frequencies (Reichardt, unpublished). With this computational background a somewhat intriguing question can now be asked: why does the circuitry detect discontinuities in the magnitude but not in the direction of motion? We refer here to the absence of discrimination in the 180° phase case of one dimensional motion; different orientations – like horizontal versus vertical – are discriminated (see Reichardt and Poggio, 1979). One possibility is that because of the high angular velocities attained by flying flies, relative motion of an object against a surround usually consists of differences in magnitude of the retinal velocities and only seldom of differences in the sign of the velocity. The circuitry of Fig. 9 implements this *via* direction independent inhibition of both progressive and regressive detectors.

Thus in the visual world of a fly, absence and presence of motion are a more reliable or simply more common cue to relative motion than discontinuities in the direction of the velocity vector. In addition, it may simply be that the 180° phase case is a side effect of a convenient hardware implementation, and almost never occurs in real life (of a fly). Whether one of these alternatives is indeed correct is a question we cannot yet answer.

7.3.5. The Circuitry as an Algorithm. In summary, the circuitry of Fig. 9, considered as an algorithm, solves a problem which has proved to be difficult in computer vision, the object-ground separation. It achieves this goal by finding discontinuities in either texture or motion from initial motion estimates that are much simpler and rougher than the precise measurement of the velocity field. In computer systems and perhaps in the human visual system such a simple detection of object boundaries may be very helpful for later computing the precise optical flow, by establishing the boundaries within which local motion measurements may be combined. In the fly's visual system a computation of the full optical flow seems at present unlikely (but see Sect. 7.3.1): only partial properties are probably computed, for instance time to landing (Wagner, 1982), other simple properties of the optical flow – like its focus – and especially motion and texture discontinuities. An extension of the circuitry to include two dimensional motion seems rather straight forward and is presently under way, together with the required behavioural experiments.

Appendix A

A.1. Presynaptic Shunting Inhibition of the Pool Cells on the Elementary Movement Detectors

Various kinds of biophysical mechanisms could underly the "gain control" inhibitory operation [see Eq. (2)], which is one of the key features of the circuitry for the detection of relative motion. Probably the simplest mechanism is presynaptic inhibition of the shunting type. We wish to outline a description of the associated "local circuit". Figure A1 shows three cell profiles which can be identified with corresponding components of the circuitry of Fig. 9a or b; (EMD: elementary movement detector, *S:* pool cell, *X:* output cell). The graded potential V_1 is induced by an excitatory input distal enough to be electrically decoupled from the site of inhibition. For simplicity, we consider in the following the steady state situation (i.e. for signals with a time course which is much "slower" than the membrane's time constant). Transient signals can be analyzed in a similar way (see Poggio and Torre, 1981: Koch et al., 1982).

Our main assumption is that inhibition is of the shunting type, which means that the synaptic signal arriving from S increases the conductance g_i to an ion (or a combination of ions) with an equilibrium potential near the resting potential of the cell ($E_i \simeq E_0$).

The membrane potential at the terminal of EMD where the output synapse is located is then

$$V_0 \sim V_1 + (E_i - V_0) g_i k_{i0} . \qquad \text{(A1)}$$

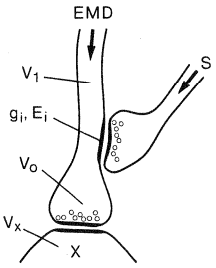

Fig. A1. An example for presynaptic inhibition of the shunting type. The graded potential V_1 is induced by an excitatory input from an elementary movement detector (EMD) distal enough to be electrically decoupled from the synaptic site of inhibition. The inhibitory synaptic signal from the pool cell S increases the conductance g_i to an ion or a combination of ions with an equilibrium potential E_i near the resting potential E_0. The membrane potential V_0 at the tip of the dendrite where the output synapse is located is then $V_0 \sim V_1 + (E_i - V_0) g_i k_{i0}$. If E_0 is defined as $E_0 = 0$, V_0 becomes $V_0 \sim \frac{V_1}{1 + g_i \cdot k_{i0}}$, where k_{i0} is the transfer resistance from the location of inhibition (i) to the location of the output synapse (0)

If $E_i \approx E_0$ and E_0 is defined as $E_0 = 0$, Eq. (A1) becomes

$$V_0 \sim \frac{V_1}{1 + g_i k_{i0}}, \qquad \text{(A2)}$$

where k_{i0} is the transfer resistance from the location of inhibition (i) to the location of the output synapse (0). Equation (A2) corresponds to Eq. (2), if $(g_i \cdot k_{i0})$ is identified with const $\cdot \sum_{i=1}^{N} x_i$. The effect of shunting inhibition is maximized by high k_{i0} values. This in turn implies that the location of inhibition (i) must be electrically near to the output synapse (0). The approach described by Poggio and Torre (1981) (see also Koch et al., 1982) can be used to analyze in detail the properties of a local circuit of this type.

A.2. The Nonlinear Operation Between the Elementary Movement Detectors and the Output Cells

The transduction between presynaptic and postsynaptic voltage is usually described as either an almost linear or a sigmoidal transformation (Katz and Miledi, 1970, and Fig. A2). In the latter case the

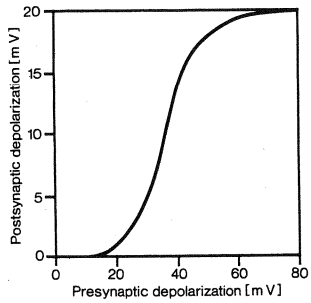

Fig. A2. Pre-postsynaptic characteristic of an excitatory synapse demonstrating the typical sigmoidal relationship between presynaptic and postsynaptic depolarization

nonlinear operation which transforms the presynaptic into the postsynaptic voltage can be approximated by a simple power as

$$V_{post} \sim V_{pre}^{n}$$

if the input signal V_{pre} is restricted to the appropriate small range of values and measured relative to a suitable reference value V_0. In particular, $V_{post} \sim V_{pre}^2$ if the input values remain in the lower range of the sigmoidal function. In the model circuitry we introduced a nonlinear synaptic transmission of this kind ($n=2$) between the elementary movement detectors EMD and the output cells X [see Eq. (3) and Fig. A1, where $U_{pre} = V_0$ and $V_{post} = V_x$].

Notice that the range compression performed by shunting inhibition on V_{pre}, is quite effective in keeping V_{pre} within a certain restricted range. Thus, shunting inhibition can effectively control the operative range of the sigmoidal function. Different values of n (like $n=1$ as introduced into the model in order to simulate the situation in *Calliphora*) can be easily obtained by shifting the "resting" value of the presynaptic potential V_0 around. Thus the parameter n – and the associated properties of the circuitry – can be easily controlled by intrinsic signals. In addition, the exact value of n is expected to be somewhat variable, given this physiological basis.

If the range of V_{pre} is too wide, approximations of the sigmoidal characteristics by a simple power become of course unsatisfactory.

Appendix B

B.1. The Forward Circuitry

The first model outlined in Chap. 4 is a representation of a neural circuitry with forward shunting inhibition. The coupled pool cells S_L and S_R summate the signals corresponding to progressive (regressive) movement in the optical environment. The outputs of the pool cells S_L, S_R are assumed to undergo a saturation effect, represented by an exponent q and to shunt each elementary movement (position) channel by presynaptic inhibition. The synapses on the X cells are assumed to operate with a nonlinear input-output characteristic which is modelled by an exponent n (see Appendix A).

We assume that the time scale characteristic for the circuitry is much faster than the time scale of the input signals. Thus we will neglect dynamic properties and consider the steady state input-output relationships.

If x_i is the signal in the i^{th} channel, then y_i, i.e. the output signal in the i^{th} channel after shunting inhibition, is given by

$$y_i = \frac{x_i}{\beta + \left(\sum_{i=1}^{N} x_i\right)^q}, \tag{B1}$$

where β is the shunting inhibition coefficient. If all input channels are equally excited (i.e. $x_i = x_j$ for all i,j), Eq. (B1) can be written as

$$y = \frac{x}{\beta + (Nx)^q}. \tag{B2}$$

Taking into account the nonlinear transformation (see Appendix A) between pre- and post-synaptic voltages and summating over all channels, the total output R takes the form

$$R = Ny^n = \frac{Nx^n}{(\beta + (Nx)^q)^n}. \tag{B3}$$

Equation (B3) does not include, of course, neither the case of relative movement (different x_i) nor the binocular connections.

The experiments with textured figures of increasing angular extent led to the conclusion that the behavioural response becomes increasingly independent of the size of the optical flow field. In terms of Eq. (B3) it means that R should become independent of N (the number of excited channels) for $(Nx)^q \gg \beta$. In this case $R \approx \frac{Nx^n}{(Nx)^{q \cdot n}}$. R is only independent of N if $q = 1/n$ so that $R \approx x^{n-1}\,\mathrm{sign}(x)$. The gain control experiment therefore relates q to n. If on the other hand $(Nx)^{1/n} \ll \beta$, we have $R \approx \frac{Nx^n}{\beta^n}$. The specific case considered in the simulation of the *Musca* behaviour is $q=0.5$ and $n=2$, implying $R \approx x$ for large N. In *Calliphora* we have to assume $q=0.5$, $n=1$ which means that the gain control condition is not strictly fulfilled. For large N the response R increases with N as $R \approx \sqrt{Nx}$.

In designing the neuronal circuitry, outlined in Fig. 9a, we have made the usual assumption that all cells carry only positive signals: In particular, channels for progressive movement are separate from channels for regressive movement. We can take the signs into account by rewriting Eq. (B3) into

$$R = \frac{Nx^n \cdot \mathrm{sign}(x)}{(\beta + (Nx)^{1/n})^n}. \tag{B4}$$

The second model described in Chap. 4 has a recurrent structure (see Fig. 9b). In the first model inhibition acts on the sensory channels after the pool cells S_L, S_R have summated the signals – the pool acts forward. In the second model the pool cells inhibit with a recurrent pathway the individual channels before they are summated in the pool cells.

We turn now to consider in more detail the recurrent circuitry.

B.2. The Recurrent Circuitry

A simple description of the recurrent network can be obtained by making the hypothesis, that the time scale of the feedback loop is "fast". More specifically, we consider in the following a specific difference equation – i.e. a discrete dynamical system – which can be associated with the recurrent circuitry of Fig. 9b. The delay in the feedback path is 1 and again the stimuli are supposed to be very slow on the time scale characteristic for the circuitry. The output of the recurrent network at time $v+1$ is, under these assumptions, for each channel

$$y_{v+1} = F(y_v) \quad \text{with} \quad F(y) = \frac{x}{\beta + (N|y|)^q} \tag{B5}$$

(all input signals are again assumed to be equal). The total output is then $R = Ny^n$.

When the recurrent system converges to one stable equilibrium, $|y_{v+1} - y_v|$ becomes smaller than ε for $v > v_\varepsilon$. The equilibrium value y^* – if it exists – is determined by $y^* = F(y^*)$. The asymptotic behaviour of the difference Eq. (B5) can be characterized completely in the following way: For certain values of the parameters in

$$\left|\left(\frac{\delta F}{\delta y}\right)_{y=y^*}\right| = \left|\frac{N^q}{x} \cdot q \cdot y^{*(q+1)}\right| < 1,$$

the discrete dynamical system is stable with an asymptotic equilibrium value given by

$$y^* = \frac{x}{\beta + (N|y^*|)^q}.$$

For

$$\left|\frac{N^q}{x} \cdot q \cdot y^{*(q+1)}\right| > 1$$

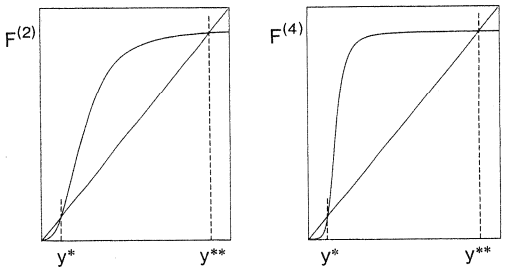

Fig. B1. Fixed points of period 2 for $F^{(2)}$ and $F^{(2n)}$ coincide

a limit circle of period 2 appears. The system does not admit any other bifurcation; neither higher order limit cycles nor chaotic behaviours are possible.

We outline the main steps of the proof. We first show that it is sufficient to consider the second iterate of the function F to characterize completely the asymptotic behaviour of our specific equation $y_{\nu+1}=F(y_\nu)$. We indicate with $F^{(n)}$ the n^{th} order iterate of F (for example $F^{(2)}[*]=F[F[*]]$).

Lemma. *Assume that $F^{(2)}$ and $F^{(2n)}$ are monotonically increasing functions with 1 diagonal crossing only (i.e. $F^{(2n)}(y)-y=0$ has only one root). Then $F^{(2n+2)}$ has only 1 diagonal crossing. If $F^{(2)}$ and $F^{(2n)}$ have 3 diagonal crossings, $F^{(2n+2)}$ has exactly 3 diagonal crossings of the same sign.*

Proof. Consider Fig. B1. The critical point is that the diagonal crossings of $F^{(2n)}$ and $F^{(2)}$ coincide (since they are fixed points of period 2). For all y such that $y^*\leqq y\leqq y^{**}$, $F^{(2n)}(y)$ is contained in the interval $[y^*, y^{**}]$ and $F^{(2n)}(y)$ in $[y^*, y^{**}]$; thus $F^{(2n)}(F^{(2)}(y))>y$ for y in the same interval. The same argument can be used for all other intervals and for the case of diagonal crossings.

For the rest of the proof we characterize the behaviour of $F^{(2)}$ for the specific function $F(y)=\dfrac{x}{\beta+(N|y|)^q}$.

Property. The function $F(y)=\dfrac{x}{\beta+(N|y|)^q}$ has a second order iterate $F^{(2)}$ which is monotonically increasing with either 1 or 3 diagonal crossings.

The function F is monotonically decreasing from $\dfrac{x}{\beta}$ (for $y=0$) to zero (for $y\to\infty$); $F^{(2)}$ is then monotonically increasing from $\dfrac{x}{\beta+\left(N\left|\dfrac{x}{\beta}\right|\right)^q}$ (for $y=0$) to $\dfrac{x}{\beta}$ (for $y\to\infty$). A sufficient and necessary condition for 3 diagonal crossings in $F^{(2)}$ is that the slope of $F^{(2)}(y)$ around the fixed point y^* is larger than 1. This occurs if and only if $\dfrac{|\delta F|}{|\delta y|}>1$ which is equivalent to $\left|\dfrac{N^q}{x}\cdot q\cdot y^{*(q+1)}\right|>1$. When $\dfrac{|\delta F|}{|\delta y|}<1$ there is only one diagonal crossing. To prove that $F^{(2)}$ cannot have more than 3 diagonal crossings, it is sufficient to show that $F^{(2)}$ has at most 1 inflection point (since $F^{(2)}$ is monotonically increasing) and crosses the diagonal at least at the fixed point y^*). We consider then the equation $\dfrac{\delta^2F^{(2)}(y)}{\delta y^2}=0$ which gives

$$\frac{2A^{-q}\cdot q^2}{q-1}=(B\cdot A^{-q}+\lambda^{-q})\left(\frac{q+1}{B}+y^{-q}\right) \tag{B6}$$

with

$$A\equiv\frac{x}{N^q};\qquad B\equiv\frac{\beta}{N^q};\qquad \lambda\equiv B+y^q.$$

The expression in the first bracket is $B\cdot A^{-q}+B^{-q}$ for $y=0$ and $B\cdot A^{-q}$ for $y=\infty$. The expression in the second bracket is ∞ for $y=0$ and $\dfrac{q+1}{B}$ for $y=\infty$. The right side of Eq. (B6) is therefore ∞ for $y=0$ and $(q+1)\cdot A^{-q}$ for $y=\infty$. Thus for $q<1$, the left side of Eq. (B6) is negative and consequently Eq. (B6) has no solution, i.e. $F^{(2)}$ has no inflection point for $q<1$. If $q>1$ Eq. (B6) has one solution if $\dfrac{2q^2}{q-1}>q+1$ which indeed is always satisfied. Thus $F^{(2)}$ has one and only one inflection point for $q>1$ [notice that each of the expressions within brackets in Eq. (B6) is a monotonic function of y].

From the previous results it is now possible to conclude that

$$y_{\nu+1}=F(y_\nu)\quad\text{with}\quad F=\frac{x}{\beta+(N|y|)^q}$$

has a stable attractor y^* for $\left|\dfrac{\delta F}{\delta y}\right|_{y=y^*}<1$ and a stable limit cycle of period 2 otherwise.

Notice that a variety of functions F lead to a second iterate $F^{(2)}$ with the relevant properties needed in the proof (see lemma). It is natural to conjecture that all monotonic decreasing $F(y)$ with a sigmoidal shape and at most 1 inflection point in $[0,\infty]$ lead to a second order iterate with either one or three diagonal crossings of the correct sign. Therefore the basic behaviour of the discrete dynamical system $y_{\nu+1}=(y_\nu)$ would not depend on the specific form but on rather general properties of F.

B.3. Comparison of Forward and Recurrent Circuitry

The simulations with the forward model shown in the paper were mainly restricted to the parameter values $n=2$, $q=0.5$. These parameters fulfill our "gain control" requirement $n\cdot q=1$, which ensures invariance of the output with respect to N for large N. What is the corresponding condition for the recurrent model, for parameter values ensuring stability?

The fixed point of the recurrent system is given by

$$y^*=\frac{x}{\beta+(N|y^*|)^q}\quad\text{or}\quad[\beta+(N|y^*|)^q]y^*=x. \tag{B7}$$

The total output of the circuitry is $R=Ny^n$. For R to become independent of N for increasing N, one obtains, for small β, $y^*=\dfrac{x}{(N|y|)^q}$ or $N^q\cdot y^{*q+1}=x$. Inserting y^* into the relation $R=Ny^n$ one has $R=N\left(\dfrac{x}{N^q}\right)^{\frac{n}{1+q}}$ which requires $q(n-1)=1$ to make R independent of N. Since $R=x$ for $q=1$, $n=2$, the equivalent parameter settings for the recurrent network are $q=1$, $n=2$. Setting $q=1$ into Eq. (B7) one obtains four solutions.

$$\begin{aligned} y_{1,2}&=\frac{-\beta\pm\sqrt{\beta^2+4Nx}}{2N}\quad\text{for}\quad y>0;\quad x>0,\\ y_{3,4}&=\frac{+\beta\mp\sqrt{\beta^2-4Nx}}{2N}\quad\text{for}\quad y<0;\quad x<0. \end{aligned} \tag{B8}$$

Only two (y_1, y_3) of them are meaningful. They can be represented together as

$$y=\frac{-\beta+\sqrt{\beta^2+4N|x|}}{2N}\cdot\operatorname{sign}(x). \tag{B9}$$

With $n=2$, and $R=Ny^2\cdot\text{sign}(x)$ Eq. (B9) gives

$$R=\frac{1}{4N}[2\beta^2-2\beta\sqrt{\beta^2+4N|x|}+4N|x|]\cdot\text{sign}(x). \quad \text{(B10)}$$

Let us now consider the two cases $4N|x|\gg\beta^2$ and $4N|x|\ll\beta^2$. From (B10) it follows

$$R\approx x \quad \text{for} \quad 4N|x|\gg\beta^2, \quad \text{(B11)}$$

$$R\approx\frac{N}{\beta^2}\cdot x^2\cdot\text{sign}(x) \quad \text{for} \quad 4N|x|\ll\beta^2. \quad \text{(B12)}$$

In spite of the fact that the structures of Eqs. (B4) and (B10) are mathematically quite different, they lead to similar solutions and cannot be separated by behavioural experiments. The solutions are, for the case considered here, similar when in the forward model n and q amount to 2 and 0.5, respectively, in the recurrent model to 2 and 1. Interestingly, the assumption of a saturation ($q=0.5$) operation of the pool output, essential for the proper operation of the forward model, can be dropped in the recurrent model ($q=1$).

Acknowledgements. We gratefully acknowledge valuable and critical remarks by H. Bülthoff, M. Egelhaaf, K. G. Götz, R. Schlögl (Frankfurt), H. Wagner, and C. Wehrhahn. We would also like to express our gratitude to L. Heimburger for skilled technical help and for drawing the figures, and to I. Geiss for typing the manuscript.

References

Baker, C.L., Braddick, O.J.: Does segregation of differently moving areas depend on relative or absolute displacement? Vision Res. **22**, 851–856 (1982)

Barlow, H.B., Levick, W.R.: The mechanism of directionally sensitive units in the rabbits retina. J. Physiol. **178**, 477–504 (1965)

Bülthoff, H.: Figure-ground discrimination in the visual system of *Drosophila melanogaster*. Biol. Cybern. **41**, 139–145 (1981)

Burr, D.C.: Temporal summation of moving images by the human visual system. Proc. R. Soc. London B **211**, 321–339 (1982)

Carpenter, R.H.S.: Movements in the eyes. London: Pion 1979

Collett, T.S.: Visual neurones for tracking moving targets. Nature **232**, 127–130 (1971)

Collett, T.S., King, A.J.: Vision during flight. In: The compound eye and vision of insects. Horridge, G.A. (ed.). Oxford: Clarendon Press 1975

Diener, H.C., Wist, E.R., Dichgans, J., Brandt, T.H.: The spatial frequency effect on perceived velocity. Vision Res. **16**, 169–176 (1976)

Eckert, H.: The horizontal cells in the lobula plate of the blowfly, *Phaenicia sericata*. J. Comp. Physiol. **143**, 511–526 (1981)

Fennema, C.I., Thompson, W.B.: Velocity determination in scenes containing several moving objects. Comp. Graph. Image Process **9**, 301–315 (1979)

Hausen, K.: Monocular and binocular computation of motion in the lobula plate of the fly. In: Verh. Dtsch. Zool. Ges. **1981**, pp. 49–70. Stuttgart: Gustav Fischer Verlag 1981

Hausen, K.: Movement sensitive interneurons in the optomotor system of the fly. I. The horizontal cells: structure and signals. Biol. Cybern. **45**, 143–156 (1982a)

Hausen, K.: Movement sensitive interneurons in the optomotor system of the fly. II. The horizontal cells: receptive field organization and response characteristics. Biol. Cybern. **46**, 67–79 (1982b)

Hausen, K., Wehrhahn, C.: Microsurgery of identified neurons of flies and their role in flight behaviour (in preparation) (1983)

Heimburger, L., Poggio, T., Reichardt, W.: A special class of nonlinear interactions in the visual system of the fly. Biol. Cybern. **21**, 103–105 (1976)

Horn, B.K.P., Schunck, B.G.: Determining optical flow. Artif. Intell. (Special Issue on Computer Vision) **17**, 185–203 (1981)

Julesz, B.: Foundations of cyclopean perception. Chicago: University of Chicago Press 1971

Katz, B., Miledi, R.: Further study of the role of calcium in synaptic transmission. J. Physiol. **207**, 789–801 (1970)

Koch, C., Poggio, T., Torre, V.: Retinal ganglion cells: functional interpretation of dendritic morphology. Philos. Trans. R. Soc. London B **298**, 227–264 (1982)

Land, M.F., Collett, T.S.: Chasing behaviour of houseflies (*Fannia canniculari*): description and analysis. J. Comp. Physiol. **89**, 331–357 (1974)

Longuet-Higgins, H.C., Prazdny, K.: The interpretation of moving retinal image. Proc. R. Soc. London B **208**, 358–397 (1980)

Marr, D.C.: Vision. San Francisco: Freeman 1982

Marr, D.C., Poggio, T.: A theory of human stereo vision. M.I.T. Artificial Intelligence Laboratory. A.I. Memo No. 451, November 1977

Marr, D.C., Ullman, S.: Directional selectivity and its use in early visual processing. Proc. R. Soc. London B **211**, 151–180 (1981)

O'Shea, M., Fraser-Rowell, C.H.: Protection from habituation by lateral inhibition. Nature **254**, 53–54 (1975)

Palka, J.: Discrimination between movements of eye and object by visual interneurons of crickets. J. Exp. Biol. **50**, 723–732 (1969)

Pierantoni, R.: A look into the cockpit of the fly. The architecture of the lobula plate. Cell Tiss. Res. **171**, 101–122 (1976)

Poggio, T.: Visual algorithms (in preparation) (1983)

Poggio, T., Reichardt, W.: A theory of pattern induced flight orientation of the fly *Musca domestica*. Kybernetik **12**, 185–203 (1973)

Poggio, T., Reichardt, W.: Visual control of orientation behaviour in the fly. Part II. Towards the underlying neural interactions. Q. Rev. Biophys. **9**, 377–438 (1976)

Poggio, T., Reichardt, W.: Characterization of nonlinear interactions in the fly's visual system, pp. 64–84. Appendix 4: A polynomial representation of algorithms, pp. 197–202. In: Theoretical approaches in neurobiology. Reichardt, W.E., Poggio, T. (eds.). Cambridge, MA, London: MIT Press 1981

Poggio, T., Reichardt, W., Hausen, K.: A neuronal circuitry for relative movement discrimination by the visual system of the fly. Naturwissenschaften **68**, 443–446 (1981)

Poggio, T., Torre, V.: A theory of synaptic interactions, pp. 28–38. Appendix 2: The mathematics of postsynaptic interaction, pp. 188–192. In: Theoretical approaches in neurobiology. Reichardt, W.E., Poggio, T. (eds.). Cambridge, MA, London: MIT Press 1981

Regan, D., Spekreijse, H.: Electrophysiological correlate of binocular depth perception in man. Nature **225**, 92–94 (1970)

Reichardt, W.: Autokorrelations-Auswertung als Funktionsprinzip des Zentralnervensystems (bei der optischen Wahrnehmung eines Insektes). Z. Naturforsch. **12b**, 448–457 (1957)

Reichardt, W.: Musterinduzierte Flugorientierung. Verhaltensversuche an der Fliege *Musca domestica*. Naturwissenschaften **60**, 122–138 (1973)

Reichardt, W., Poggio, T.: Visual control of orientation behaviour in the fly. Part I. A quantitative analysis. Q. Rev. Biophys. **9**, 311–375 (1976)

Reichardt, W., Poggio, T.: Figure-ground discrimination by relative movement in the visual system of the fly. Part I. Experimental results. Biol. Cybern. **35**, 81–100 (1979)

Reichardt, W., Poggio, T.: Visual control of flight in flies. In: Theoretical approaches in neurobiology. Reichardt, W., Poggio, T. (eds.). Cambridge, MA, London: MIT Press 1981

Richards, W., Lieberman, H.R.: Velocity blindness during shearing motion. Vision Res. **22**, 97–100 (1982)

Srinivasan, M.V., Dvorak, D.R.: Spatial processing of visual information in the movement-detecting pathway of the fly. J. Comp. Physiol. **140**, 1–23 (1980)

Torre, V., Poggio, T.: A synaptic mechanism possibly underlying directional selectivity to motion. Proc. R. Soc. London B**202**, 409–416 (1978)

Virsik, R., Reichardt, W.: Tracking of moving objects by the fly *Musca domestica.* Naturwissenschaften **61**, 132–133 (1974)

Virsik, R., Reichardt, W.: Detection and tracking of moving objects by the fly *Musca domestica.* Biol. Cybern. **23**, 83–98 (1976)

Wagner, H.: Flow-field variables trigger landing in flies. Nature **297**, 147–148 (1982)

Wehrhahn, C.: Sex-specific differences in the chasing behaviour of houseflies *(Musca).* Biol. Cybern. **32**, 235–241 (1979)

Wehrhahn, C.: Fast and slow flight torque responses in flies and their possible role in visual orientation behaviour. Biol. Cybern. **40**, 213–221 (1981)

Wehrhahn, C., Poggio, T., Bülthoff, H.: Tracking and chasing in houseflies *(Musca).* An analysis of 3-D flight trajectories. Biol. Cybern. **45**, 123–130 (1982)

Received: January 17, 1983

Prof. Dr. W. Reichardt
Max-Planck-Institut für
biologische Kybernetik
Spemannstrasse 38
D-7400 Tübingen
Federal Republic of Germany